Maxime Mussard

A solar concentrator with heat storage and self-circulating liquid

Thesis for the degree of Philosophiae Doctor

Trondheim, September 2013

Norwegian University of Science and Technology
Faculty of Engineering Science and Technology
Department of Energy and Process Engineering

NTNU – Trondheim
Norwegian University of
Science and Technology

NTNU
Norwegian University of Science and Technology

Thesis for the degree of Philosophiae Doctor

Faculty of Engineering Science and Technology
Department of Energy and Process Engineering

ISBN 978-82-471-4437-4 (printed ver.)
ISBN 978-82-471-4438-1 (electronic ver.)
ISSN 1503-8181

Doctoral theses at NTNU, 2013:164

Printed by NTNU-trykk

Preface

This thesis is submitted in partial fulfillment of the requirements for the degree of Philosophiae Doctor at the Norwegian University of Science and Technology (NTNU).

The doctoral work has been carried out at the Department of Energy and Process Engineering of NTNU, under the supervision of Professor Ole Jørgen Nydal and co-supervision of Emeritus Professor Jørgen Løvseth.

Acknowledgments

Working with solar energy was my motivation for attending this PhD, and I will never be grateful enough to my supervisor Professor Ole Jørgen Nydal for trusting me and giving me the chance to work with him. His kindness and availability made things much more easier, and his experience and advices were undoubtely necessary to guide this work through these four years.
I would like to express my greatest gratitude to all the trainees, masters, PhDs and professors of the NUFU solar oven project, both in Norway and Africa. It was a pleasure to meet our African friends yearly and participate to all these constructive meetings. I would like to thank particularly my co-supervisor Professor Emeritus Jørgen Løvseth for his countless advices; my colleagues Habtamu Bayera Madessa and Chee Woh Foong for providing momentum and knowledge to start my PhD in the best conditions; and my colleague Pia Piroshka Otte for sensibilizing me on the social aspects of solar cooking and keeping me entertained all along our work travels.

My experiments could not have been completed without the help and advices of some of the technicians of the EPT department; and the administrative support from Anita Yttersian and Gunhild Valsø Engdal was simply excellent.
I gratefully acknowledge the professors of the department, especially Professors Odilio Alves-Filho and Olav Bolland, for their support and availability.
Special thanks to all the PhDs and employees of the department for sharing great times such as PhD meetings, running time, or simply random discussions to keep our minds awake.

I would like to thank as well Alexandre Morin for distracting my mind during our countless coffee breaks.

And last but not least, thank you to Heike Hoedt and Wolfgang Scheffler for sharing with us their invaluable experience on solar cooking, both on the technical and socio-economical aspects.

Abstract

The main objective of this thesis is to design and test a solar concentrating collector with heat storage for domestic applications, mainly solar cooking. The system must be cheap, robust, easy to use and maintain, and non-hazardous. The system must be able to store energy over 200°C to enable cooking, baking and frying. The heat collection is performed with a parabolic trough focusing the energy on a focal line where the absorber stands, the whole system is driven with a solar tracker.

The first task is to find relevant materials for heat storage. After investigation, latent heat materials show a better potential for this application, especially for their ability to store a lot of energy at constant temperature.
The influence of solar tracking inaccuracy is investigated as well, and shows that by chosing a large absorber, it is possible to both reduce the influence of these inaccuracies and of the solar angle.

The concept of self-circulation has numerous advantages, such as the absence of a pumping system and the self-regulation of the temperature. This concept is then tested with a first prototype to ensure that it is suitable for our objectives. The test shows a great ability for thermal oil to transfer energy from the collector to a heat storage placed above using the self-circulation principle.
The next objective is then to optimize the heat transfer into the absorber. After comparing with electrical heating the performance of two different storages coupled with the same self-circulating loop, it appears that a storage with a larger volume of oil is more efficient than an aluminum-based storage. Coupled with latent heat materials, the oil-based storage is then the basis for the following tests.

Experiments are conducted outdoors to test the charging of the system with the sun. Absorbers with and without insulation are tested, and as expected the insulation (air layer) around the absorber is necessary to reach quickly high temperatures. The system proves to be good enough to charge a storage in one sunny day starting from ambient temperature. The energy stored is large enough to provide cooking energy for two people.
After charging, heat extraction experiments are conducted. The system shows great abilities for frying but boiling water takes time. After testing with a

flat plate, it appears that the low quality of the contact between the top plate and the cooking pan contributes to the long cooking time. By improving the flatness of the top of the heat storage, boiling water can be performed in a reasonable time, competitive compared to traditional cookings devices or commercialized direct solar cookers.
A final test was started with an evacuated tube around the absorber, and simulations on the upscaling of the storage are made to conclude on the potential of this concept.
The measurements have successfully been compared with a dynamic system model. The computational model was used for upscaling analysis.

Contents

1. Introduction

This chapter introduces the thesis by describing general aspects of the main subjects discussed in the thesis and an associated literature review. First, a background concerning solar energy and especially solar cooking is given. It is followed by a discussion on the different ways of storing heat; the principle of self-circulation is then detailed, and to finish issues concerning sun tracking and ray tracing are discussed.

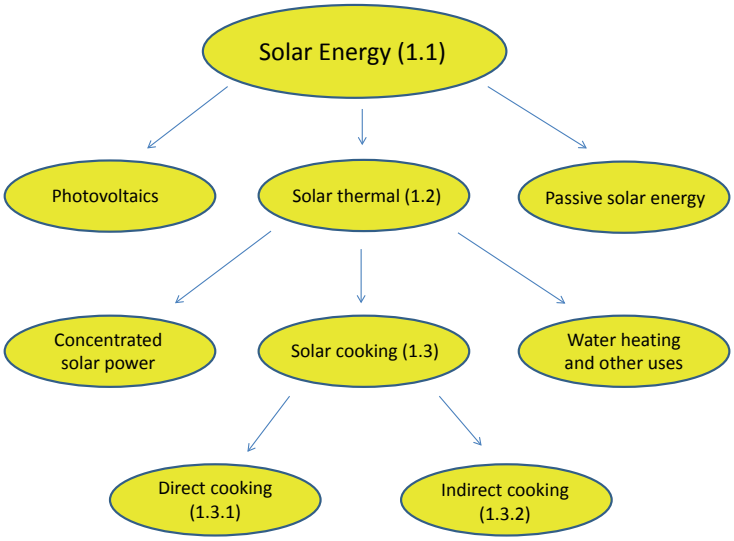

Figure 1.1.: The different uses of solar energy

1.1. Solar energy conversion

The sun gives to the earth in about 2 to 4 hours [1] the total energy consumption of the global world population in one year [2]. However, despite its potential, the part of solar energy in the total energy consumption is still very low. There is different ways of using solar energy, the simplest and most

natural one is the passive heating. Optimization of this process can be done while studying for example passive houses or low-emissions buildings [3]. A second way of using solar energy is to convert it directly to electricity with photovoltaic panels. This technique is nowadays widely used but the efficiency can still be improved [4]. Finally, using the heat of the sun directly as thermal energy is another way of using this energy.

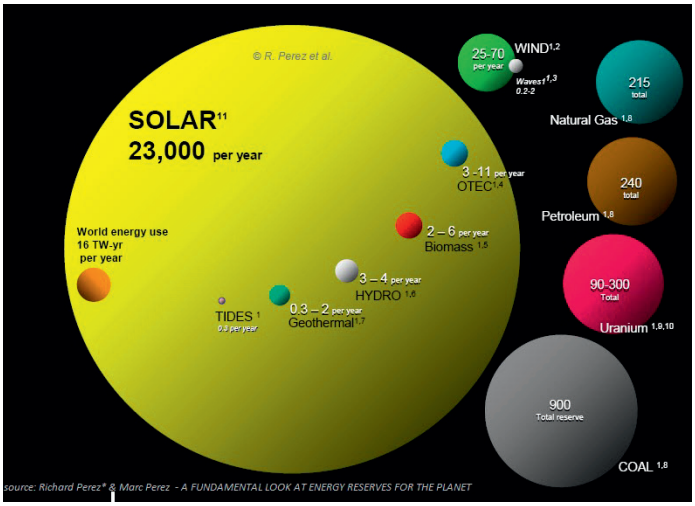

Figure 1.2.: Potential of solar energy compare to other renewable energies (yearly), and fossil fuels (total) [5]

1.2. Solar thermal energy use

Converting solar energy for direct use as thermal energy is rather simple and typically done for hot water domestic systems [6], solar drying [7], solar sterilization [8] and many other applications. It is possible as well to use this thermal energy to run a turbine and produce electricity, like in the Concentrating Solar Power plants (CSP). Three technologies are mainly developed nowadays: the power plants made of parabolic troughs [9]; the heliostat systems coupled with a tower [10]; and the collectors directly coupled with a Stirling engine [11].

Solar cooking is another interesting way to use solar energy.

Figure 1.3.: Domestic hot water solar heater, CSP power plant with parabolic troughs, solar tower with heliostats, and parabolas with Stirling engines [12]

1.3. Solar cooking

Many different solar cookers have been implemented with more or less success since the years 1970. The majority of them are direct solar cookers; some indirect systems have been developed as well [13]. This part shows a non-exhaustive list of solar cookers.

1.3.1. Direct solar cookers

The simplest and most effective way of transferring the energy from the sun to the application is direct heating. The different kinds of direct solar cookers are presented here.

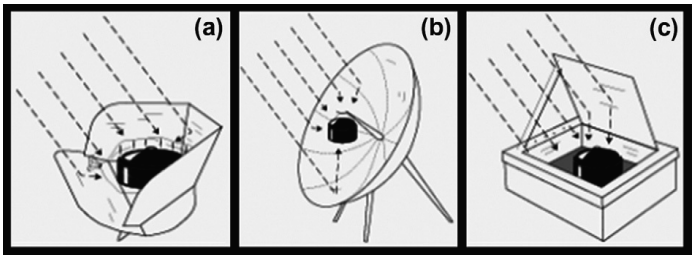

Figure 1.4.: Direct solar cookers: with panels (a), parabolic (b) or box (c) [13]

Box cookers

There are many different kinds of box cookers, but the principle remains the same: the box is oriented towards the sun, the rays of the sun enter through a window covering the top of the box and the energy is absorbed due to dark painting. Mirrors can increase the performance and it is possible to reach about 130°C [14].

Figure 1.5.: Solar box cooker [13]

Concentrating cookers

To increase the concentration and the temperature, the use of a reflective structure is necessary. Using panels is a simple and effective option to increase the performance. By using a parabolic shape, the focusing can be optimized such that the cooking plate temperature can reach 180°C [15].

Figure 1.6.: Solar parabola for cooking and frying purposes [15]

The Scheffler solar cooker is a direct solar cooker suitable for any type of cooking. Its fixed focus principle makes it attractive despite a certain technical complexity. A 1-axis tracking coupled with a seasonal adjustment of the shape of the parabola is necessary [16].

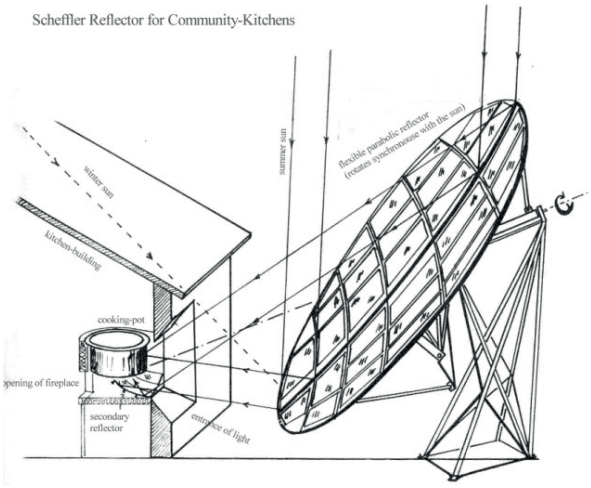

Figure 1.7.: Scheffler solar cooker [16]

1.3.2. Indirect solar cookers

With an indirect solar cooker, it is either possible to cook in a separate place (for example indoor), or to store energy during sunshine to use later in the day (evening, night, or the following day). For example, systems coupled

with one or several Scheffler reflectors have been studied for small and large scales.

Schwarzer cooker

This cooker is based on a self circulating loop filled with peanut oil, carrying the energy from a flat collector (with lateral mirror panels) to the application (heat storage or cooking vessel) using peanut oil as a heat transfer fluid [17]. The system enables cooking at 140°C.

Figure 1.8.: Schwarzer solar cooker [17]

Scheffler reflector with heat storage

The Scheffler reflector is perfectly suitable to concentrate the energy on a heat storage (made of melting tin, iron or aluminum) during the day to use this energy later when there is no sunshine anymore [18].
With a set of these reflectors, it is possible to produce and store pressurized steam at about 150°C. The solar kitchen at Mount Abu (India) works with this principle. It can feed 20 000 people per day and is the largest solar kitchen in the world.

Figure 1.9.: Solar kitchen in Mount Abu [19]

Spherical solar cooker

The spherical solar cooker developed in Auroville, India, can generates steam for cooking for 1 000 people per day [20]. The energy focuses on a central receiver where steam is produced.

Other heat storage based cookers

Many other prototypes coupled with heat storage have been developed. These system can store energy up to 120°C during some hours [21], using direct heating of the storage or heat pipes.

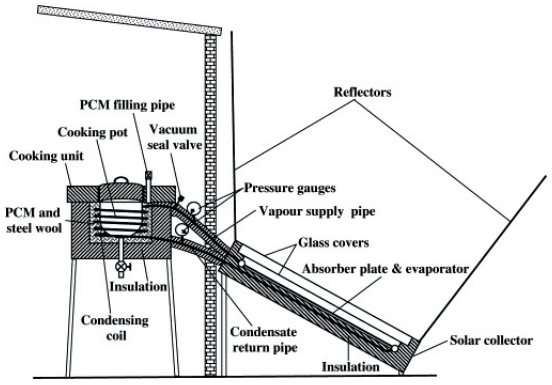

Figure 1.10.: Solar cooker: flat plate collector coupled with a heat storage [22]

1.4. Heat storage

As we can see, a thermal storage can significantly increase the performance and competitiveness of a solar installation. Solar irradiation is intermittent and irregular, so a storage can correct this variations to optimize the use of the energy collected.

1.4.1. Sensible heat

The simplest way of storing thermal energy is to use the sensible heat of the material. This principle is widely used and studied. These materials can in general be cheap, chemically stables and easy to manipulate. Water, rocks, iron or oil are common sensible heat storage media. Many of them have an increasing heat capacity with temperature, which make them an interesting option for storing energy. However, if this point is relevant for a large range of functional temperature [23], it is more difficult to get energy at a constant temperature.

The heat storage potential of a given material is given by the formula:

$$Q = \int_{T_1}^{T_2} mC_p dT \tag{1.1}$$

Where Q is the total amount of energy stored [J];
m is the mass of the medium [kg];
C_p is the specific heat of the medium, potentially temperature dependent [J/kg.K];
T_1 and T_2 are the initial and final temperatures of the relevant range [K].

A sensible heat storage (rock based) coupled with a solar collector has been tested at NTNU [24].

1.4.2. Latent heat

Using latent heat due to phase change is an efficient way of storing heat. It allows storing a significant amount of energy at constant temperature, making the use of the energy more predictable. Typically, during a solid-liquid phase change, the fusion absorbs energy while the solidification releases it. The heat storage potential of the phase change materials (PCM) is important,

commonly equivalent to over 100°C of sensible heat of the same material [25]. Typical latent heat storage materials are: tin, steraic acid, combination of nitrate salts, etc. The operational temperature range of the application must include the melting temperature to optimize the system.

These materials have more constraints than the sensible heat materials due to the phase change [26, 27], so it is important to take into account the new parameters involved with the melting (chemical reactivity, sealing, thermal expansion, etc.). Many latent heat options have been studied for low [25, 26] or higher [28] melting temperatures.

The energy storage for a range of temperature including the melting point is:

$$Q = \int_{T_1}^{T_m} mC_p dT + mh + \int_{T_m}^{T_2} mC_p dT \tag{1.2}$$

Where Q is the total amount of energy stored [J];
m is the mass of the medium [kg];
C_p is the specific heat of the medium (solid below T_m, liquid over), potentially temperature dependent [J/kg.K];
h is the latent heat [J/kg];
T_m is the melting temperature, T_1 and T_2 are the initial and final temperatures of the relevant range [K].

The nitrate salts are commonly used for latent heat storage coupled with solar energy. A prototype of heat storage using $KNO_3 - NaNO_3$ (40:60 molar ratio) with direct solar heating has been tested at NTNU by Foong [29].

1.4.3. Thermochemical storage

The principle of a thermochemical heat storage is to use the energy from an exothermic reaction for the application, and charge the storage by running the corresponding endothermic reaction. The storage potential of the thermochemical energy is very important, but the technical limits are nowadays too high to be suitable for a low-cost solar cooking system. However, improvements and research are intensively conducted both for large size seasonal [30] and small size modules [31] and may lead to extremly interesting solutions.

1.5. Self-circulation

Using the self-circulation principle is an interesting option. A fluid driven by gravity difference does not necessitate the use of a pump and a well-designed system will then regulate its temperature by itself. This principle is already widely used, for example in the thermosyphon solar hot water systems [32].

The self-circulation is based on the Darcy-Weisbach equation [33]:

$$\frac{\Delta P}{L} = \lambda \rho \frac{U^2}{2} \frac{1}{D} \tag{1.3}$$

In this expression, L is the length of the section, D its diamter, ρ is the density of the fluid, U the velocity and ΔP the pressure drop, with:

$$\Delta P = \Delta \rho g h \tag{1.4}$$

$\Delta \rho$ is the density difference between the upward and downward parts, g the standard gravity and h the height of the column of liquid.
And λ is the Darcy friction factor for laminar flows, expressed as [34]:

$$\lambda = \frac{64}{Re} = \frac{64\mu}{\rho D U} \tag{1.5}$$

where Re is the Reynolds number and μ the dynamic viscosity.

This formula is applicable for a system where all the pipes have the same diameter. For a system with different pipe diameters, after development of the equation and introduction of the volumetric flow M_v (m^3/s), the equation becomes:

$$M_v = \frac{gh\pi.\Delta\rho}{128\mu \sum L/D^4} \tag{1.6}$$

The pressure drops due to elbows or other imperfections can be expressed as a pipe length equivalent.

1.6. Sun tracking and ray tracing

Tracking the sun is necessary for concentrating systems. While some simple direct cookers just need a manual adjustment every 20 minutes, the concentrating systems need an accurate system to keep the collector perpendicular to the rays of the sun [24]. The tracking can be manual, mechanical or electronic. A 1-axis system is sufficient during one day if the cooker is oriented North-South, but a seasonal tracking is compulsory for parabolic dish systems, but not necessary for a parabolic trough.

A daily tracking needs to rotate at constant speed and covers 180° in 12 hours, so the rotational speed is:

$$\omega = 15^\circ/hour \tag{1.7}$$

The different tracking orientations are represented in Figure 1.11.

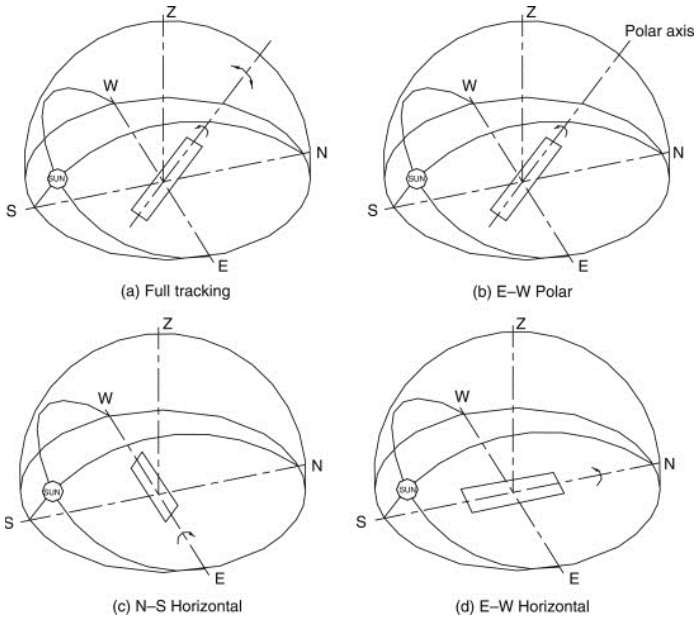

Figure 1.11.: Different tracking orientations [35]

Except the optimum full tracking, the other tracking orientations have different efficiencies for an horizontal surface (Figure 1.12).

From this graphics, we can see that for a flat surface, the EW polar tracking is more efficient than the NS horizontal (but more demanding for mechanical

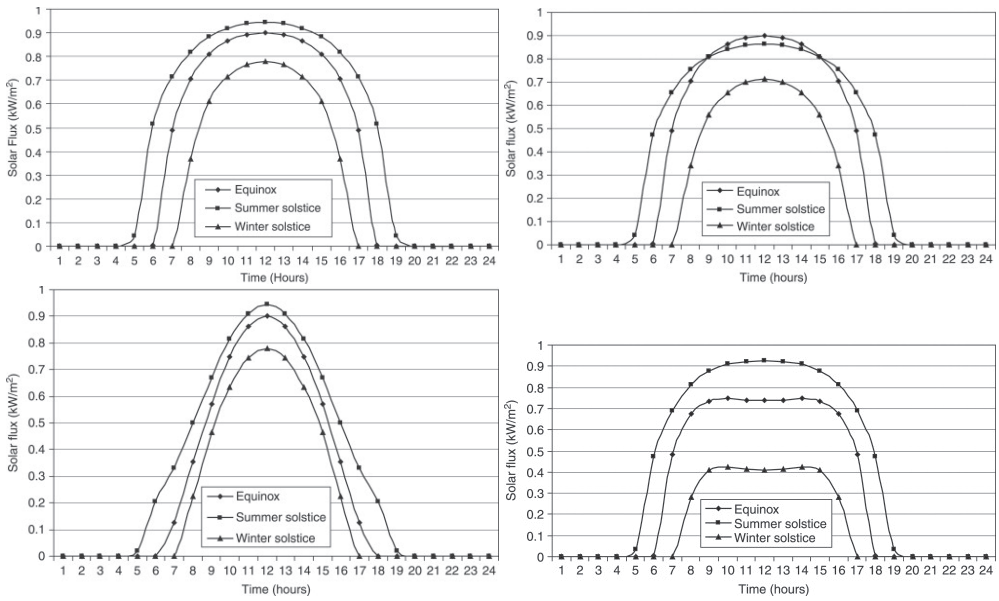

Figure 1.12.: Heat collection: full tracking, and with 1-axis tracking: E-W Polar, N-S horizontal, and E-W horizontal (35°North) [35]

constraints) and the EW horizontal. For a small single parabolic trough, that is even more important to have the rays as perpendicular to the collector as possible, so the polar axis orientation seems to be the most interesting choice. A further investigation related to the latitude of the place may be relevant to do before installing a solar collector in the field.

Ray tracing can help to improve the understanding of the behaviour of the sun rays. The system and its collector experimented during this thesis were simulated by a ray tracer programmed at NTNU using C++.

1.7. Heat collection

1.7.1. Solar concentrating systems

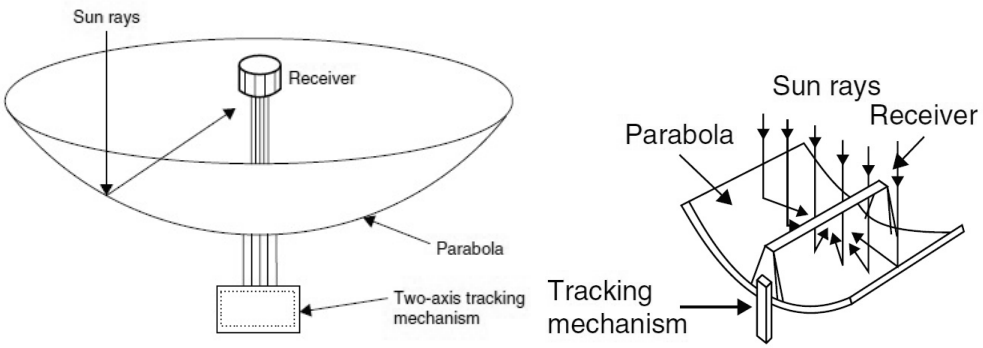

Figure 1.13.: Parabolic dish (left) and trough (right) principles [36]

A concentrating system with tracking can be based on two principles:
- Using a parabolic dish, the rays of the sun focus on one point. High temperatures can be reached due to the high concentration ratio, but a two-axis tracking is mandatory. Furthermore, it is more complex to make, and the high focusing can be dangerous.

- Using a parabolic trough, the rays of the sun focus on a focal line. The temperature range is limited due to the lower concentration ratio. However, a trough is easier to make and maintain, and there is a much lower burning or overheating risk. Even if a 2-axis system is optimum, a 1-axis system can be sufficient.

Due to its advantages and the relatively low constraints concerning the temperatures, the option of the parabolic trough is chosen as a solar collector for the storage.

Figure 1.14 summarizes the characteristics of different energy collectors (the concentration ratio is define in part 1.7.2).

Motion	Collector type	Absorber type	Concentration ratio	Indicative temperature range (°C)
Stationary	Flat-plate collector (FPC)	Flat	1	30–80
	Evacuated tube collector (ETC)	Flat	1	50–200
	Compound parabolic collector (CPC)	Tubular	1–5	60–240
Single-axis tracking			5–15	60–300
	Linear Fresnel reflector (LFR)	Tubular	10–40	60–250
	Cylindrical trough collector (CTC)	Tubular	15–50	60–300
	Parabolic trough collector (PTC)	Tubular	10–85	60–400
Two-axis tracking	Parabolic dish reflector (PDR)	Point	600–2000	100–1500
	Heliostat field collector (HFC)	Point	300–1500	150–2000
Note: Concentration ratio is defined as the aperture area divided by the receiver/absorber area of the collector.				

Figure 1.14.: Characteristics of different solar energy collectors [36]

1.7.2. Geometry of a parabolic trough

Shape of the parabola

The shape of a parabola is defined by the equation $y^2 = 4fx$, where f is the focal length. a is the aperture of the trough and ϕ_r is the rim angle, as

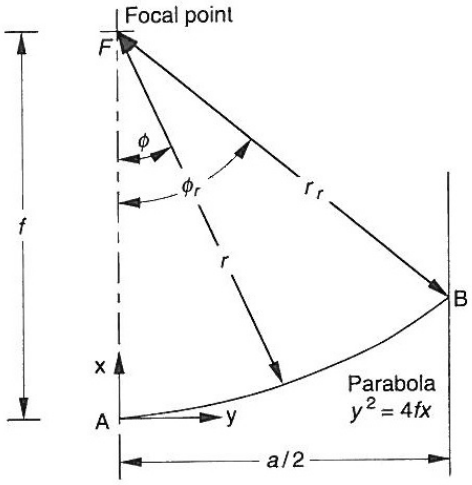

Figure 1.15.: Section of a linear parabolic concentrator [37]

described in Figure 1.15. For the experiments, the following data can be applied: a = 1 m; ϕ_r = 100°; f = 0.2 m. A wide rim angle is chosen to keep the center of mass as close as possible to the absorber, facilitating the balancing of the system.

Size of the absorber

According to Figure 1.16 and to the dimensions defined previously, an absorber tube with a diameter w of 4.6 mm is theoretically necessary to collect the sun rays under perfect conditions, considering a solar angle of 32'. For our experiments, a diameter of 22 mm is chosen; a good balance between optimal collection (tolerating tracking inaccuracy), low friction, low thermal losses, avoiding of overheating, sufficient concentration ratio (cf 1.7.3) and availability of materials.

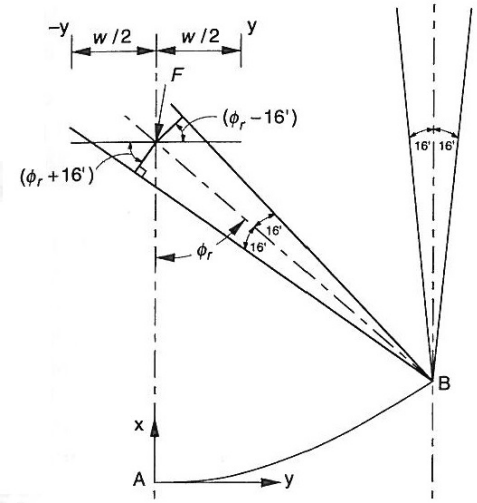

Figure 1.16.: Image dimension for a parabolic trough [37]

Concentration ratio

The concentration ratio is define by [37]:

$$C = \frac{A_a}{A_r} \tag{1.8}$$

where A_a is the aperture of the collector, and A_r is the area of the absorber. While an optimized system could theoretically lead to a concentration ratio of 70, our system has an average concentration ratio around 15 on the absorber surface. It is theoretically possible to reach temperatures about 300°C on the absorber [37].

1.8. List of papers

Five papers were accepted for publication in international journals (two of them are going to be presented during an international conference). In addition, two papers have been presented during international conferences. The secondary authors are Ole Jørgen Nydal (programming of the ray tracer in paper B, discussion and critical comments for the other papers), Erwan Vaujany (experimental and simulation work in paper C) and Alexandre Gueno (experimental and simulation work, and partial writing of the paper F).

Paper A
Assessments of the thermal storage potential of sensible and latent heat-based systems for solar domestic applications
Authors: Maxime Mussard, Ole Jørgen Nydal
Published in: *Proceedings of the 7th International Renewable Energy Storage Conference and Exhibition, Berlin, Germany.*
Year: 2012

Paper B
Influence of solar tracking inaccuracy and sun rays modeling on the efficiency of a small-scale solar parabolic trough
Authors: Maxime Mussard, Ole Jørgen Nydal
To be presented at: *ISES World Solar Congress 2013, Cancún, Mexico.*
Accepted for publication in: *Energy Procedia*
Year: 2013

Paper C
Heating of an oil-based heat storage with a low-cost small-scale solar parabolic trough
Authors: Maxime Mussard, Erwan Vaujany, Ole Jørgen Nydal
Published in: *Proceedings of the EuroSun2012 - ISES Europe Solar Conference, Rijeka, Croatia.*
Year: 2012

Paper D
Comparison of oil and aluminum-based heat storage charged with a small-scale solar parabolic trough
Authors: Maxime Mussard, Ole Jørgen Nydal
Published in: *Applied Thermal Engineering*, Volume 58, Issues 1-2, September 2013, Pages 146-154.
Year: 2013

Paper E
Charging of a heat storage coupled with a low-cost small-scale solar parabolic trough for cooking purposes
Authors: Maxime Mussard, Ole Jørgen Nydal
Published in: *Solar Energy*, Volume 95, September 2013, Pages 144-154.
Year: 2013

Paper F
Experimental study of solar cooking using heat storage in comparison with direct heating
Authors: Maxime Mussard, Alexandre Gueno, Ole Jørgen Nydal
Accepted for publication in: *Solar Energy*
Year: 2013

Paper G
Solar cooker with heat storage at high temperature: charging experiments and simulations
Authors: Maxime Mussard
To be presented at: *ISES World Solar Congress 2013, Cancún, Mexico.*
Accepted for publication in: *Energy Procedia*
Year: 2013

2. Methodology

2.1. Motivation

Many direct solar cookers already exist and all of them are able to heat food (70°C), many of them can boil water (100°C), and some of them can be used for frying (over 160°C). There are as well cookers with heat storage, where the heat is stored during the day and used during the evening. The Schwarzer cooker enables cooking at pretty high temperatures even during storage charging, but is limited for high temperature frying such as Injera Baking [17, 15]. The Scheffler reflector enables this kind of frying, but not during the charging time; furthermore the heat losses are not optimized, the system is massive and may be difficult to manipulate for a non-trained person.
The main motivation of this work is to build and design a solar cooker which can store energy at high temperatures to enable any kind of cooking (including frying at high temperatures), and can be used during charging as well if necessary. The system has to be cheap, robust, made with non-toxic materials; and easy to make, use and maintain.

2.2. Objectives

The objectives of this work are the following:
- Decide on the best materials to use for heat storage (Paper A);
- Investigate the ray tracing concerning a parabolic trough (Paper B);
- Conclude on the feasibility of a self-circulation system coupled with a heat storage and a mechanical tracking (Paper C);
- Find the optimal storage combination between heat transport, storage and thermal conductivity (Paper D);
- Test and simulate the charging of an optimized storage coupled with a parabolic trough and an electronic tracking (Paper E);
- Test and simulate the heat extraction for both boiling and frying, and compare with existing devices (Papers E and F);

- Optimize the design of the absorber, especially its insulation (Papers E and G);
- Conclude with simulations concerning the upscaling potential of the system (Paper G).

2.3. Description of the system

The system is made of a self-circulating loop coupled with a solar parabolic trough. The heat storage and heat exchange inside the storage vary between the different tests. The absorber can be insulated or not.

2.3.1. Self-circulating loop

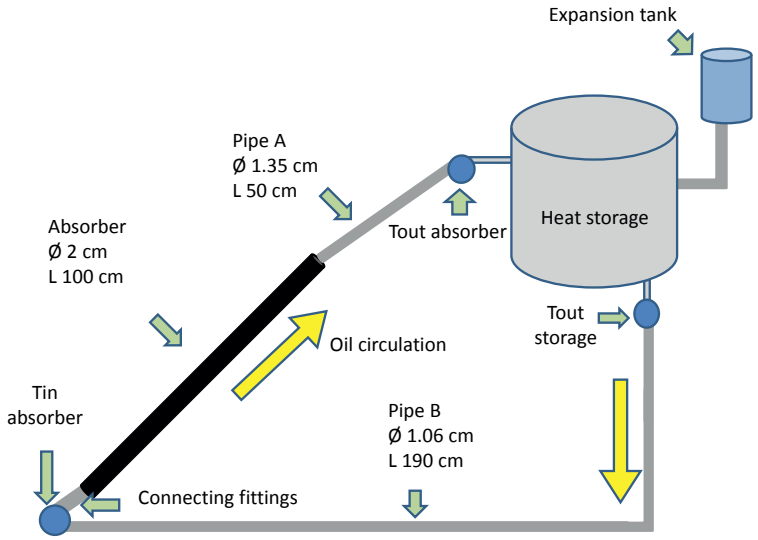

Figure 2.1.: Self-circulating loop

The loop is filled with a heat transfer oil (Syltherm 800, Duratherm FG or Duratherm 630). The sun is heating the oil through the absorber: the oil gets then lighter and starts circulating, the circulation is governed by the friction/gravity balance around the loop. Once it reaches the storage, a heat exchange occurs,

the oil is then cooled and comes back to the absorber. An opening to the atmosphere is necessary to control the oil expansion.

2.3.2. Heat storage

Nitrate salts are chosen for the storage, due to their heat capacity, easy availability and manipulation, and low cost. To optimize the heat conduction, aluminum is used due to its high heat conductivity and reasonable price and weight.

2.3.3. Tracking system

Two daily tracking systems were tested during the thesis work (a mechanical clockwork and an electronic-based tracker, both inspired from a design by W. Scheffler).
The system was inclined below the polar axis due to mechanical constraints (around 45°), and to be closer to the seasonal orientation during summer.

2.3.4. Collector

The two collectors tested and used are an aluminum sheet covered with a reflective film, and a flexible mirror from Alanod (90% reflectivity).

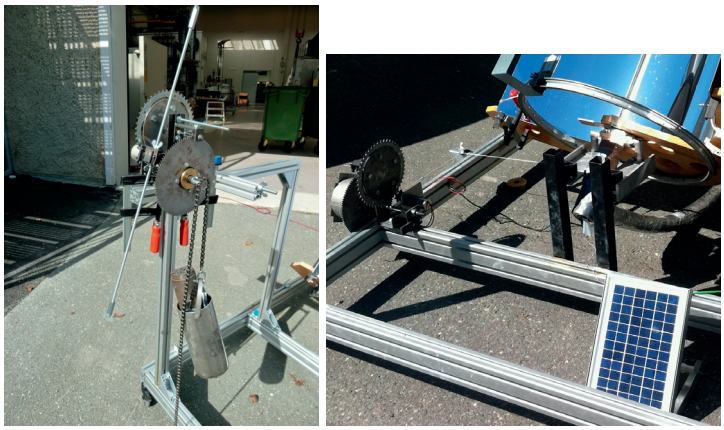

Figure 2.2.: Mechanical and electronic tracking systems tested

2.4. Experiments and simulations

2.4.1. Experiments

The outdoor experiments are conducted in Trondheim, Norway.

Self-circulation testing

Figure 2.3.: Spiral running inside the storage

A first experiment shows the relevance of the self-circulation coupled with a solar parabolic trough (Paper C). The storage is filled with avocado oil, the loop is filled with Syltherm 800 and the heat exchange occurs on a spirale inside the heat storage.

Storage performance comparison

A second experiment is conducted indoor to compare two storage designs (Paper D). The self-circulating loop is then filled with Duratherm FG (cheaper and more resistant to high temperatures [38, 39]):
- The first system couples the same loop with an aluminum-based storage: channels are drilled through the aluminum block, and cylinders contain the PCM (nitrate salts) ;
- The second storage is oil-based, the heat transfer oil is flowing directly into a cylindrical container where aluminum cylinders filled with PCM are immersed.

Figure 2.4.: Aluminum and oil-based storage structure

The second system proved to be more efficient and this concept is used and tested for the next experiments.

Absorber insulation comparison

The importance of the insulation around the absorber is then discussed in papers E and G. Outdoor tests are run with different insulations (without insulation, with air layer, and preliminary test with evacuated tube) under sunny conditions and the results are compared. These tests are run using Duratherm 630 as a heat transfer fluid (an evolution of Duratherm FG with better heat resistance).

Extraction tests

Once the storage is charged, boiling and frying are tested. A comparison with a direct solar cooker and surface contact optimization using an electrical plate are conducted as well and detailed in papers E and F.

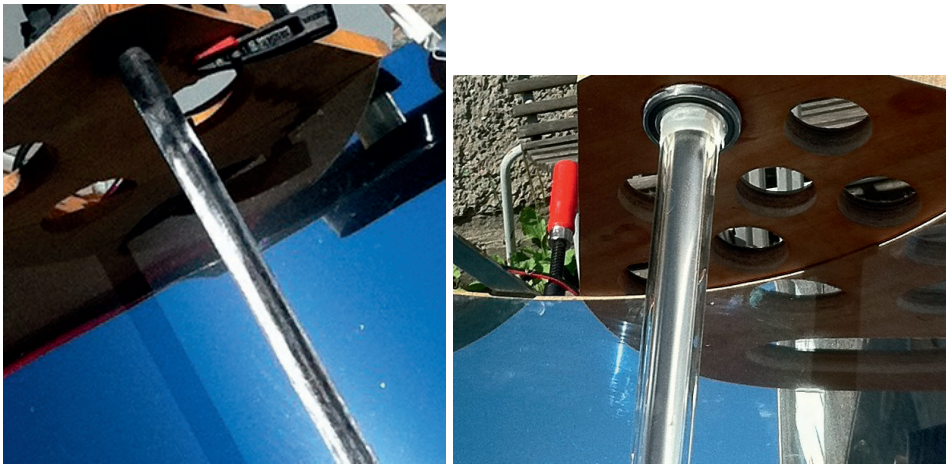

Figure 2.5.: Absorber without and with insulation

2.4.2. Ray tracing

By using a ray tracer (Paper B), the behaviour of the rays of the sun can be visualized. For example, the two next pictures show a difference of behaviour between a 0.5 cm diameter absorber getting rays with 0.5° inclination, and a 2 cm diameter with 0.8° inclination.

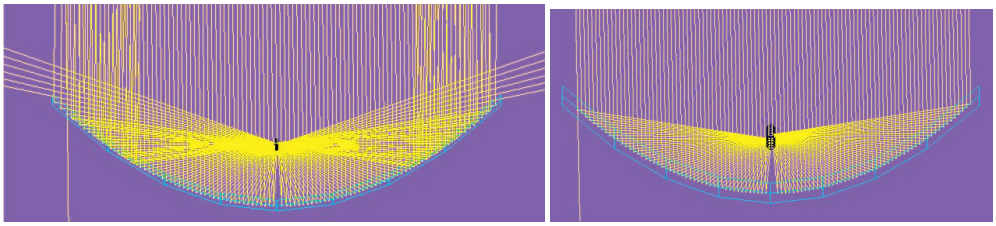

Figure 2.6.: Ray tracing for two absorber diameters: 0.5 cm (0.5°), and 2 cm (0.8°)

2.4.3. Self-circulation model

The thermal behaviour of the system is simulated using the finite-volume method.

Conservation equation The energy balance for a given cell is [40]:

$$\frac{\partial \rho C_p T}{\partial t} + \frac{\partial \rho C_p T U}{\partial x} = \frac{Q_{source} - Q_{losses}}{V} \tag{2.1}$$

where ρ is the density of the heat transfer fluid (kg/m^3), C_p the heat capacity (J/kg.K), T the temperature (K), U the velocity of the fluid (m/s), V is the volume of a given cell (m^3), Q_{source} (W) is the thermal gain for the cell (nul except at the absorber), Q_{losses} (W) is the sum of the losses for the cell. These losses are detailed below.

Losses by convection/conduction around the absorber tube If the absorber tube is not protected and directly exposed to air circulation, the losses by convection are represented by the coefficient h_c (W/m^2.K). We have then [40]:

$$Q_{conv} = h_c(T - T_0)A \tag{2.2}$$

where A is the area of the cell (m^2), T is the temperature of the cell and T_0 the ambient temperature (K).

If the tube is insulated the conduction through this insulation is considered.

The air layer is approximated as a free-convection cell, which facilitates the use of the Nusselt number Nu. Losses by conduction through the glass at the extremities are considered as well for the two cells at the extremities [40]:

$$Q_{cond} = (\frac{Nu 2\pi L_{abs}\lambda_{air}}{ln(\frac{Do_{abs}+l_{air}}{Do_{abs}+e_g})} + \lambda_g Do_{abs}\pi l_g/e_g)(T - T_0) \tag{2.3}$$

where λ_{air} (W/m.K) the conductivity of the air, L_{abs} is the length of the absorber, Do_{abs} is the outside diameter of the absorber, l_{air} the air layer thickness, e_g the glass thickness, l_g the length of the glass bridge between the two walls (all distances in meters) and T_0 the ambient temperature. If the double-wall glass tube is evacuated below 1 Pa, the conduction between the walls is divided by a factor 4 [41], the expression of the conduction through the two glass bridges remains the same.

Losses by radiation from the absorber The absorber is the only heated part of the system not protected by solid insulation, radiation from other parts are then not considered. The Stefan-Bolzmann equation is then used [42], where σ is the Stefan-Bolzmann constant:

$$Q_{rad} = \epsilon\sigma(T^4 - T_0^4)\pi L_{abs} Do_{abs} \tag{2.4}$$

When the glass tube is around the absorber, a part of the radiation losses is reflected back or absorbed due to the two glass walls. The reflectivity of the glass must be then taken into account.

Losses by conduction The pipes of the self-circulating loop and the storage are covered with insulation, the conduction equation used are [43]:

$$Q_{condc} = \frac{2\pi L_{cell}\lambda_{insul}}{ln(\frac{R2}{R1})}(T - T_0) \tag{2.5}$$

for cylindrical geometries, with L_{cell} length of the cell, λ_{insul} conductivity of the insulation, $R2$ and $R1$ the outside and inside radius; and:

$$Q_{condf} = \lambda_{insul}\frac{S}{e}(T - T_0) \tag{2.6}$$

for flat geometries, with S area and e thickness of the insulation.

Finite-volume method Applying the equations described below for the heat losses (Q_{losses}), it is then possible to compute the temperature using the finite-volume method. After discretizing the system in cells, the general expression for a cell n of the absorber at an instant t is:

$$T(t,n) = T(t-1,n).(1-\frac{M_v\Delta t}{V_{cell}})+T(t-1,n-1).\frac{M_v\Delta t}{V_{cell}}+T(P_{sun})-T(Q_{losses}) \tag{2.7}$$

where M_v is the volumetric mass flow (m^3/s), V_{cell} the volume of a given cell, Δt is the time step (1 s), $T(P_{sun})$ the temperature increase due to the energy reflected from the solar collector and $T(Q_{losses})$ the temperature drop due to the thermal losses (both in K).

For the other cells of the loop (storage included), the term expressing the gain from the collector disappear and the expression becomes:

$$T(t,n) = T(t-1,n).(1-\frac{M_v \Delta t}{V_{cell}})+T(t-1,n-1).\frac{M_v \Delta t}{V_{cell}}-T(Q_{losses}) \quad (2.8)$$

By running a simulation, it is possible to visualize the simulated temperature at any point of the loop in time, and compare to the experimental data.

2.4.4. Heat extraction simulation using COMSOL

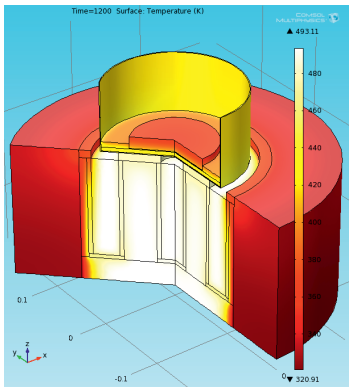

Figure 2.7.: Use of Comsol: temperature of the components for a frying test after 20 minutes

The software Comsol Multiphysics is a powerful tool which includes heat conduction analysis using the finite element method. By simulating a heat extraction process, the behaviour of the storage and the application can be represented with color gradient.

3. Summary of papers

The different aspects on the work are explained in the articles. This part details the main points of each paper.

Paper A: Assessments of the thermal storage potential of sensible and latent heat-based systems for solar domestic applications

A comparison between two sensible (iron, graphite) and latent heat-based materials (tin, nitrate salts) is detailed. The latent heat shows a greater heat storage potential for our range of temperature (180 to 250°C). Furthermore, due to its reduced size at equivalent heat storage potential, a latent-heat based heat storage needs much less energy for the preheating to the operational temperature. The system is then much quickly operational compare to a sensible-based storage.

Paper B: Influence of solar tracking inaccuracy and sun rays modeling on the efficiency of a small-scale solar parabolic trough

Using a ray tracer, the sensitivity of a parabolic solar trough is tested. The rays of the sun are first considered parallel; then the influence of the solar angle is modeled with a specific discretization of the sun. It is shown that the solar angle has a certain influence and should be taken into account, especially for small absorber diameters. Having a large absorber will reduce its influence and the global sensitivity of the system to tracking inaccuracy.

Paper C: Heating of an oil-based heat storage with a low-cost small-scale solar parabolic trough

An experimental work is conducted and described here. The main objective is to test a first prototype to validate the feasability of a self-circulating system. A solar parabolic trough is coupled with a closed self-circulating loop starting at the absorber. The storage is filled with avocado oil and Syltherm 800 is used as heat transfer fluid. The loop passes through a spiral inside the storage where the heat exchange takes place. Despite the lack of optimization, the system proved to be efficient enough and the results are promising. A first model is programmed to simulate the efficiency of the system, and different improvement options are tested.

Paper D: Comparison of oil and aluminum-based heat storage charged with a small-scale solar parabolic trough

The objective of this paper is to compare two heat storage designs.
The first one is mainly made of aluminum with cavities for nitrate salts: the aluminum stores the heat and spread the energy all over the storage, while the salts optimize the heat storage around 220°C. Channels are drilled for driving the heat transfer fluid (Duratherm FG) through the storage.
The second one is mainly made of heat transfer fluid. Aluminum cylinders sealed on the lid and containing nitrate salts are immersed into the oil. Despite the aluminum cylinders, the heat conductivity is much lower than in the first storage. However, the friction is lower as well and stratification is expected at the bottom of the storage. The two systems have a similar heat capacity.
After running experiments and simulations, the oil-based storage is proved to be about two times more effective than the aluminum-based one.

Paper E: Charging of a heat storage coupled with a low-cost small-scale solar parabolic trough for cooking purposes

Charging experiments with an oil-based storage with aluminum cylinders filled with salts are conducted. For the first experiment, the absorber is not insulated at all; while in the second experiment, a double wall glass tube containing air is protecting the absorber from heavy losses. The two versions are tested under similar sunny conditions. The glass protecting the absorber is proved to be more efficient, and is required in order to reach the melting temperature of the salts. Simulations show that the main benefit is the reduction of convective losses, despite the importance of optical losses due to the two glass walls. With the glass absorber, the storage can be fully charged with the sun in 6 hours. Discharging and cooking tests are conducted as well.

Paper F: Experimental study of solar cooking using heat storage in comparison with direct heating

This paper focuses on the heat extraction. A boiling test is conducted: the fully charged storage can boil 1 liter of water in about 38 minutes. By improving the contact area, it is proved experimentally that the boiling time can be reduced to 16 minutes. This result shows that the system is competitive compared to commercially available solar cookers (comparison with SK 14). Frying is tested as well and the experiment is successful. Simulations are made to confirm the hypothesis and visualize the heat extraction.

Paper G: Solar cooker with heat storage at high temperature: charging experiments and simulations

Starting from the model described in the previous papers, upscaling of the system is tested. Based on assumptions of the performance of the system coupled with an evacuated absorber, a demonstration of the storage potential under these conditions is made. According to the simulations, the energy stored can be drastically increased after careful optimization of the system.

4. Conclusion and recommendations

4.1. Conclusion

The conclusions of the thesis work related to the objectives described in 2.2 are detailed here.

For a reduce range of operational temperatures (about 50°C), the latent heat-based materials are more effective for storing heat than the sensible heat systems. Their high heat capacity around their melting point reduces the size of the storage and the energy necessary to heat the system to the operational temperature. Furthermore, as the systems are potentially smaller, it is easier and cheaper to insulate, move and use them in general.
Using a large absorber tube can help to correct the potential tracking or collector inaccuracies, also due to the slightly non-parallel solar rays.
The self-circulation is an elegant way of transporting heat from a collector to a heat storage: there is no need of a pump and the system regulates itself. However it necessitates suitable heat transfer fluids and careful optimization of the friction (pipes diameter and length). Keeping the absorber without insulation avoids overheating of the heat transfer oil but decreases the performance.
For a cooker working with self-circulation, a heat storage mainly made of oil is more efficient than an aluminum-based one. Despite a slower heat transfer inside the storage, the oil circulates faster (less friction), and combined to a slight stratification at the bottom of the storage it leads to significantly increased performances.
The charging of the storage under sunshine is possible up to 200°C with a 1 m^2 collector without insulating the absorber, and this option is even optimal to charge around 100°C. However, insulation is necessary to reach more than 200°C. An air layer around the absorber tube is sufficient to melt enough nitrate salts (220°C) in 5 hours to cook for a couple of people.
The heat extraction is feasible on the storage (both boiling and frying), but an optimized contact (type electrical cast iron cooking plate) is necessary to be competitive regarding traditional cooking devices.

Coupled with an evacuated tube, the experimental setup is underscaled but the concept shows a great potential of heat collection and storage.

4.2. Recommendations

The main recommendations concern the long-term testing of the system. Concerning mechanical robustness, too little experiments have been done to conclude on this.
Experience is lacking concerning the durability of the heat transfer oil in the system. The influence of the sealing (to avoid contact with the atmosphere and oxydation) on the life expectancy of the oil can be investigated. Furthermore, other oils are available and it would be useful to test many of them to find the most suitable. Temperature tolerance experiments for laminar flows can be of an interest.
The influence of the pipe diameters on the fluid life expectancy can be investigated as well, in particular regarding the maximal temperature reached in the absorber, and if this temperature has an influence on the durability of the fluid.
The behaviour of the oil in the pipes and in the storage could be studied to have a better understanding of the fluid mechanics of the system.
Concerning the storage, oil and salts must be well separated and a risk assessment is necessary.
A storage with tin could be tested with this system. Tin is more stable and efficient than salts, but heavier and more expensive.
The use of an evacuated insulation around the absorber needs careful optimization. Further investigations concerning the reduction of the pressure drop and/or the reduction of the concentration ratio should be done. Others heat-resistant oils can be tested as well.
An optimized storage surface could be designed, for example by using an electrical cast iron plate. Circulating oil to the application can be an interesting option.
According to the simulations, improving the coating on the absorber may slightly increase the performance and could be investigated, as well as reducing the diameter of the absorber for increasing the concentration ratio. The use of commercially available evacuated tubes may be an option.
A new storage with a higher heat storage potential may be design coupled with an evacuated tube around the absorber. Increasing the diameter of the pipes may be a solution to avoid overheating of the heat transfer oil.

Upscaling of the system needs further studies, investigations on a longer absorber and/or a lower declination can be made as well.
The wire-based automatic tracking system seems robust and accurate enough.

Bibliography

[1] M. Collares-Pereira and A. Rabi. The average distribution of solar radiation-correlations between diffuse and hemispherical and between daily and hourly insolation values. *Solar Energy*, 22:155–164, 1979.

[2] Z.M. Chen and G.Q. Chen. An overview of energy consumption of the globalized world economy. *Energy Policy*, 39:5920–5928, October 2011.

[3] H. Chan, B. Riffat, and J. Zhu. Review of passive solar heating and cooling technologies. *Renewable and Sustainable Energy Reviews*, 14:781–789, 2010.

[4] B. Parida, S. Iniyan, and R.Goic. A review of solar photovoltaic technologies. *Renewable and Sustainable Energy Reviews*, 15:1625–1636, 2011.

[5] solarenergyfactsblog.com. last access: January 2013.

[6] S. Jaisankar, j. Ananth, S.Thulasi, S. Jayasuthakar, and K. Sheeba. A comprehensive review on solar water heaters. *Renewable and Sustainable Energy Reviews*, 15:3045–3050, 2011.

[7] K. Jairaj, S. Singh, and K. Srikant. A review of solar dryers developed for geape drying. *Solar Energy*, 83:1698–1712, 2009.

[8] N.K. Bansal, R.L. Sawhney, A. Misra, and A. Boettcher. Solar sterilization of water. *Solar Energy*, 40:35–39, 1988.

[9] A. Giostri, M. Binotti, M. Astolfi, P. Silva, E. Macchi, and G. Manzolini. Comparison of different solar plants based on parabolic trough technology. *Solar Energy*, 86:1208–1221, 2012.

[10] M.A. dos Santos Bernardes and T.W. von Backstrom. Evaluation of operational control strategies applicable to solar chimney power plants. *Solar Energy*, 84:277–288, 2010.

[11] B. Kongtragool and S. Wongwises. A review of solar-powered stirling

engines and low temperature differential stirling engines. *Renewable and Sustainable Energy Reviews*, 7:131–154, 2003.

[12] www.jc-solarhomes.com. last access: January 2013.

[13] E. Cuce and P.M. Cuce. A comprehensive review on solar cookers. *Applied Energy*, 102:1399–1421, 2013.

[14] A. Saxena, A. Varun, S.P. Pandey, and G. Srivastav. A thermodynamic review on solar box type cookers. *Renewable and Sustainable Energy Reviews*, 15:3301–3318, 2011.

[15] A. Gallagher. A solar fryer. *Renewable and Sustainable Energy Reviews*, 85:496–505, 2011.

[16] A. Munir, O. Hensel, and W. Scheffler. Design principle and calculations of a scheffler fixed focus concentrator for medium temperature applications. *Solar Energy*, 84:1490–1502, 2010.

[17] K. Schwarzer and M.E. Vieira da Silva. Characterisation and design methods of solar cookers. *Solar Energy*, 82:157–163, 2008.

[18] M. Gotz. Liquid tin heat storage for scheffler parabolic cookers. *www.cuisinesolaire.com/E/Benicarlo03.htm*, Last access: January 2013.

[19] www.ecofriend.com. last access: January 2013.

[20] J van den Akker and J. Lipp. The power of human unity: Renewable energy in auroville. *Refocus*, 5:26–29, 2004.

[21] A. Sharma, C.R. Chen, V.V.S. Murty, and A. Shukla. Solar cooker with latent heat storage systems: A review. *Renewable and Sustainable Energy Reviews*, 13:1599–1605, 2009.

[22] H.M.S. Hussein, H.H. El-Ghetany, and S.A. Nada. Experimental investigation of novel indirect solar cooker with indoor pcm thermal storage and cooking unit. *Energy Conversion and Management*, 49:2237–2246, 2008.

[23] M.E. Navarro, M. Martinez, A. Gil, A.I. Fernandez, L.F. Cabeza, R. Olives, and X. Py. Selection and characterization of recycled materials for sensible thermal energy storage. *Solar Energy Materials and Solar Cells*, 107:131–135, 2013.

[24] H.B. Madessa. *Investigation of Small Scale Solar Concentrating Parabolic Dish with Heat Storage*. NTNU, 2011.

[25] M.K. Rathod and J. Banerjee. Thermal stability of phase change materials used in latent heat energy storage systems: A review. *Renewable and Sustainable Energy Reviews*, 18:246–258, 2013.

[26] S. Khare, M. Dell'Amico, C. Knight, and S. McGarry. Selection of materials for high temperature latent heat energy storage. *Solar Energy Materials and Solar Cells*, 107:20–27, 2012.

[27] H.E.S. Fath. Technical assessment of solar thermal energy storage technologies. *Renewable Energy*, 14:35–40, 1998.

[28] H. Michels and R. Pitz-Paul. Cascaded latent heat storage for parabolic trough solar power plants. *Solar Energy*, 81:829–837, 2007.

[29] C.W. Foong. *Experimental and numerical investigations of a small scale double-reflector concentrating solar system with latent heat storage*. NTNU, 2011.

[30] T. Li, R. Wang, J.K. Kiplagat, and Y. Kang. Performance analysis of an integrated energy storage and energy upgrade thermochemical solid-gas sorption system for seasonal storage of solar thermal energy. *Energy*, In Press:1–14, 2013.

[31] A. Abedin and M. Rosen. Assessment of a closed thermochemical energy storage using energy and exergy methods. *Applied Energy*, 93:18–23, 2012.

[32] S.V. Joshi, R.S. Bokil, and J.K. Nayak. Test standards for thermosyphon-type solar domestic hot water system: review and experimental situation. *Solar Energy*, 78:761–798, 2005.

[33] E. Romeo, C. Royo, and A. Monzon. Improved explicit equations for estimation of the friction factor in rough and smooth pipes. *Chemical Engineering Journal*, 86:369–374, 2002.

[34] D.D. Joseph and B.H. Yang. Friction factor correlations for laminar and transition and turbulent flow in smooth pipes. *Physica D*, 239:1318–1328, 2010.

[35] S.A. Kalogirou. *Solar thermal systems: Components and Applications*. Elsevier, 2012.

[36] S.A. Kalogirou. Solar thermal collectors and applications. *Progress in Energy and Combustion Science*, 30:231–295, 2004.

[37] J.A Duffie and W.A. Beckman. *Solar engineering of thermal processes*. Wiley, 2006.

[38] Duratherm Extended Life Fluids. Duratherm FG. *Available at: www.heat-transfer-fluid.com*, 2012. Last access: 23/11/12.

[39] Loikits Distribution LTD HTF. Syltherm 800. *Available at: www.loikitsdistribution.com*, 2012. Last access: 04/02/13.

[40] W. Kays, M. Crawford, and B. Weigand. *Convective Heat and Mass Transfer*. McGraw Hill, 2005.

[41] J. Wang, X. Huang, G. Cong, M. Hao, and F. Yin. A systematic study of the residual gas effect on vacuum solar receiver. *Energy Conversion and Management*, 32:2367–2372, 2011.

[42] M.F. Modest. *Radiative Heat Transfer*. McGraw Hill, 2003.

[43] Y. Cengel. *Heat and Mass Transfer*. McGraw Hill, 2005.

A. Assessments of the thermal storage potential of sensible and latent-heat based systems for solar domestic applications

Maxime Mussard, Ole Jørgen Nydal

Proceedings of the 7th International Renewable Energy Storage Conference and Exhibition, Berlin, Germany. November 2012.

Assessments of the thermal storage potential of sensible and latent heat-based systems for solar domestic applications

Maxime Mussard, Ole Jørgen Nydal

Department of Energy and Process Engineering, Norwegian University of Science and Technology, Kolbjørn Hejes vei 1D, Trondheim, Norway

Abstract

In this paper, different options for high temperature thermal storage are described and compared. The main objective is to store the heat collected during the day by a small scale solar concentrator, and then use the storage as a cooker or dryer (or any other application) during the night or a cloudy following day. The system is liquid-based: the collector concentrates the energy on the receiver so that the fluid inside the receiver is heated and can carry the energy to the storage. This study focuses essentially on the heat storage capacity of differents materials. The range of temperature studied here is between 180 and 250°C. A comparison between the best sensible heat materials (iron, carbon) and melting materials (nitrate salts, tin) is realized to conclude on the relevance of latent heat-based system compare to sensible heat-based ones.

Keywords: heat storage, latent heat, sensible heat, heat capacity

Email address: maxime.mussard@ntnu.no (Maxime Mussard, Ole Jørgen Nydal)

1. Introduction

Solar cookers convert solar radiation into heating energy. They have been designed and developed since the years 1970[1][2][3][4], to reduce the use of others non-renewable energies (charcoal, wood, fuel) in sunny areas. There is now a large variety of solar cookers, but most of them concentrate the energy of the sun directly on the food container. The use is then limited to the sunny days of the warm areas. To improve the development of the solar cookers, the use of a heat storage is then necessary: it will allow to cook during the night and/or cloudy meteorological conditions. Nowadays, two ways of storing heat through materials are commonly used: the sensible heat and the latent heat. This study focuses on this two ways of storing energy at high temperatures.

2. Objectives

The heat of the storage is suppposed to be used for multipurpose applications, but the main objective is to design a storage able to give enough energy to fry a certain amount of food. The target here is the baking of Injera, a traditional bread of easter Africa. The frying temperature can reach 180°C[5] or more, so the objective is to store as much energy as possible over this temperature. Furthermore, for these purposes, it is not worthwhile to store energy over 250°C: it is difficult to reach this temperature, the losses will increase and the temperature will be too high to fry[5]. The useful temperature range is then between 180 and 250°C. Furthermore, when two systems have the same size and insulation, the one with the highest energy density will store more energy. By using a high energy density material, the storage becomes smaller for the same efficency (and the smaller size reduces the insulation cost). Getting a compact system will then be a secondary objective. The comparison of the volumetric heat storage potential is then considered more relevant than the massic one.

3. Background

The energy stored in any single material can take two different forms: the sensible heat and the latent heat. To compare this two different kind of storages, it is important to remember that:
- Any element of the storage must reach 180°C before being useful
- The storages must be compared at equal useful energy E stored

3.1. Materials choice

The objective now is to compare the thermal properties of different materials. Different storages are considered, each made with 100 % of a material. They are all able to store the same amount of thermal energy between 180 and 250 °C.

3.1.1. Choice of the latent heat materials

Two candidates are interesting and investigated here: the Potassium-Sodium nitrate salts (KNO_3-NaNO_3) called salts later in this article, and tin. The melting temperatures are between 210 and 220°C for the salts[6] and 232°C for tin[7].

3.1.2. Choice of the sensible heat materials

For the sensible heat materials, two differents materials will be studied: iron, which has been chosen because of its high volumetric and slightly increasing sensible heat regarding the temperature[7]; and graphite, because of its significantly increasing sensible heat regarding the range of temperature [7].

3.2. Heat capacity

The main parameter which will influence the comparison of differents materials in this paper is the heat capacity C_p. For the salts, we consider the latent heat h_l as a part of the heat capacity. Here are the formulas and values used (T in Kelvins):
Graphite[7]:
$C_p = 17,15 + 4,27.10^{-3}T - 8,79.10^5T^{-2}$ J/mol.K
Iron[7]: $C_p = 17,49 + 24,77.10^{-3}T$ J/mol.K
Tin[8]: $C_p = 178+1,7.10^{-1}T$ J/kg.K; $h = 58,5$ kJ/kg; C_p considered constant after melting (negligible influence)
Salts (melting included, in kJ/kg.K)[6]:

$$C_p = \begin{cases} 1 & \text{if } T < 383 \\ 4{,}128 & \text{if } 383 \leq T \leq 393 \\ 1{,}6 & \text{if } 393 < T < 483 \text{ and } T > 493 \\ 12{,}463 & \text{if } 483 \leq T \leq 493 \end{cases}$$

3.3. Sensible heat

The sensible heat is the simplest way of storing energy, many materials have been investigated[9][10][11].

The energy stored is then:

$$E = m \int_{T_1}^{T_2} C_p dT$$

where m is the mass of the storage.

If C_p is considered constant or averaged between this range of temperature:

$$E = mC_p\Delta T$$

with:

$$\Delta T = T_2 - T_1$$

In this paper, $T_1 = 180°C$ and $T_2 = 250°C$. Knowing E, ΔT and C_p, m can be computed. Notice that, as E and ΔT are constant, mC_p is equal for all sensible heat materials. It implies that if the objective is to reduce the mass of a sensible heat storage system, a system with high sensible heat has to be chosen.
However, a sensible heat system needs to be heated up to 180°C before getting useful energy. At constant heat capacity, a lot of energy is necessary to heat between T_0=40°C (if it is the starting temperature) and T_1=180°C, before collecting useful energy between T_1 and T_2=250°C. If 250°C is the limit, it means that the fraction of the time lost to heat is:

$$r = \frac{T_1 - T_0}{T_2 - T_0}$$

So r=$2/3^{rd}$ of the collecting time (and energy) is used to heat to the operational temperature T_1. However it can be improved with a good insulation (then T_0 increases, which slows down the cooling after use).
This estimation is done considering C_p constant; however, in this large range of temperature, the heat capacity of some materials (carbon, iron[8]) can increase significantly. It is then necessary to consider in the computation the average heat capacity for each range of temperature (heating and useful range). The objective is then to have a heat capacity as low as possible under 180°C (to reduce the heating energy necessary) and as high as possible over 180°C (to reduce the mass and volume, and store more energy). Then the global ratio between efficient heating and total heating can be improved.

Now, by writing the previous equation in volumetric terms, it becomes:

$$E = VC_{p_{vol}}\Delta T$$

with V volume of the system; and the energy density $C_{p_{vol}}$ equals to:

$$C_{p_{vol}} = \rho C_p$$

where ρ is the density of the material.

As for the massic equation, E and ΔT are constant, so $VC_{p_{vol}}$ is constant for any sensible heat materials (C_p constant or averaged). As a high heat capacity reduces the mass, a high energy density will then reduce the volume.

3.4. Latent heat

A system based on latent heat is more complex: a phase change material (PCM) is melted, so it implies physical constraints. This way of storing energy has been studied at low temperatures[9][12][13][14], or high temperatures[6]. Regarding the conditions fixed previously, the materials must have a melting temperature in the working range, so between 180 and 250°C. However, the latent heat is very efficient (equal to sometimes more than 100°C temperature difference of sensible heat[8]). Furthermore a lot of energy at constant temperature is then available. And the heating time to 180°C will be then potentially reduced compare to a sensible heat material, due to the reduced quantity of material. For a latent heat material, the energy stored is then:

$$E = m(h_l + \int_{T_1}^{T_2} C_p dT)$$

with the same conditions than for the sensible heat system, and the melting point between T_1 and T_2. A system with high h and C_p will then be potentially more compact.

With C_p constant (or averaged), and in volumetric terms, it becomes:

$$E = V(h_{vol} + C_{p_{vol}}\Delta T)$$

With: $C_{p_{vol}} = \rho C_p$ and $h_{vol} = \rho h_l$

4. Methodology

4.1. Comparison of the materials

The storage has to be preferably compact and light. As described previously, the compacity is more important than the lightness, due to insulation reduced cost, increased efficiency and of course smaller volume. The first step is then to compare the storage potential of one liter of each material between the chosen temperature range, by computing the energy storable in each material volume unit, knowing C_p and h_l.

4.2. Sizing of the storages

To get an idea of the quantity of energy to store, an objective must be fixed. Baking an injera bread needs 83 kJ[5]; in addition the half of this energy is necessary to heat the pan or keep it warm[5], an approximate baking energy chosen for the computations is then E_b=125 kJ per bread. The consumption is around one bread per day per person[5]. Furthermore, the storage must cover the cooking and heating needs after the sunset or during a cloudy day. The storage will be designed to cook n=40 breads, which can cover the cooking and others uses of a community during one day. The total energy E_t which must be stored over 180°C is then:

$$E_t = E_b.n$$

We get then E_t=5 MJ. The objective is then to design systems able to store 5 MJ between 180°C and 250°C. By dividing E_t by the amount of energy stored in one liter, the volume necessary for each storage is then easily obtained.

4.3. Comparison of the efficiency of the storages

From that computation, storage sizes are obtained for the different materials tested. All these storages have now the same storage potential between the range of temperature chosen. The parameters which will change between the different options are then the volume and the weight.

A certain amount of energy is necessary to reach the operational temperature. This energy can be considered as useless for the chosen purpose, so this is an important parameter that must be reduced as much as possible. The energy necessary to heat to the operational temperature are computed for each storage. The efficiency of each storage (ratio r between the useful energy and the sum of the useful and heating energy) will be inversely related to that heating energy.

4.4. Comparison of the behaviour of each storage

To visualize the behaviour of the different storages, the temperature of each storage regarding the time (during charge) are represented. The most efficient storages are the one which get full first. Then, the useful energy available during the charging is drawn.

5. Results

5.1. Storage potential

The thermal energy density of each material between 180°C and 250°C is drawn here. The Figure 1

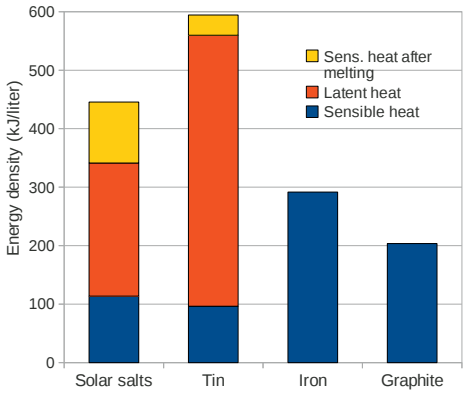

Figure 1: Thermal energy density (kJ/liter) between 180 and 250°C

shows the huge gain of energy due to the latent heat for salts and tin. As the range of temperature chosen here is reduced, the sensible heat-based materials are globally not as effective as the latent heat ones.

5.2. Comparison of the systems at equal storage potential

Knowing the energy density of each material, the interest is now to compare them at equal storage potential.

5.2.1. Sizing of the storage

As explain previously, a simple computation give us the volume for each storage necessary to store a identical amount of energy. For 5 MJ, the volumes needed are then 11.3 liters of salts, 8.41 of tin, 17.1 of iron or 24.6 liters of graphite.

5.2.2. Importance of the previous heating

Knowing the volume needed for each candidate, it is then possible to compute the energy necessary to heat each system up to the operational temperature. The starting temperature is 40°C here, and the objective is to reach 180°C. The computations are represented in Figure 2.

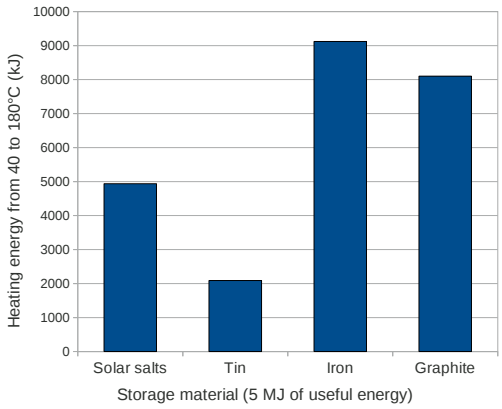

Figure 2: Heating energy necessary from 40 to 180°C, for a 5 MJ storage made of each material

The Figure 2 shows one of the other advantages of the latent heat compare to the sensible heat-based systems: the heating energy (and so the heating time) is several times smaller than for the sensible heat system. It is really significant for the tin; for the salts, it is less important due to a first endothermic modification below 180°C[6]. It is then faster to reach the operational temperature for these two materials.
The efficiency of each storage can be expressed as:

$$r = \frac{Useful\ energy}{Total\ energy}$$

where $Total\ energy$ is the sum of the heating energy (represented in Figure 2) and $Useful\ energy$, which is by definition 5 MJ.

By computing r, we get then the efficiency of each storage for a starting temperature of 40°C (i.e the time used to charge the storage between 180°C and 250°C, over the total time needed):

- Salts: $r = 51\%$
- Tin: $r = 71\%$
- Iron: $r = 35\%$
- Carbon: $r = 38\%$
- Sensible heat material with C_p constant: 33%

A material with a very low heat capacity under 180°C and very high over this temperature would have an efficiency close to 100%.

5.2.3. General behaviour of the system

To complete the study, the evolution of the behaviour of each system is drawn in Figure 3, under a 1 kW heating and considering uniform heating. As expected with the previous results, it is possible to see that the total heating time is much shorter for the latent heat-based system. All the storages have by definition the same heating time from 180 to 250°C (5000 seconds to reach 5 MJ for a 1 kW heating).

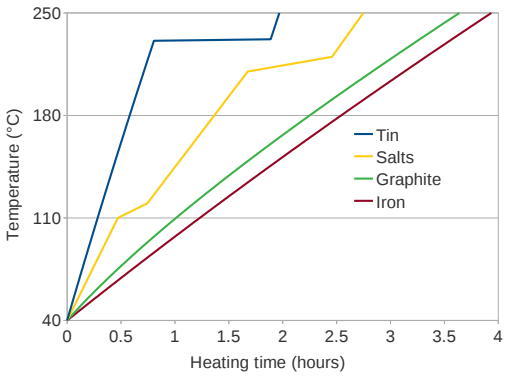

Figure 3: Evolution of the temperature in each storage, for a heating power of 1kW, starting at 40°C

5.2.4. Useful energy stored

From the previous datas, it is then possible to draw the useful energy available for each storage along the time, starting at 40°C, under a heating power of 1 kW. By reaching quickly the operational temperature, the latent heat-based systems begins to store useful energy before the sensible heat system (neglecting the heat conductivity). It is interesting to notice that the latent heat-based storages are full before the iron storage begins to store useful energy.

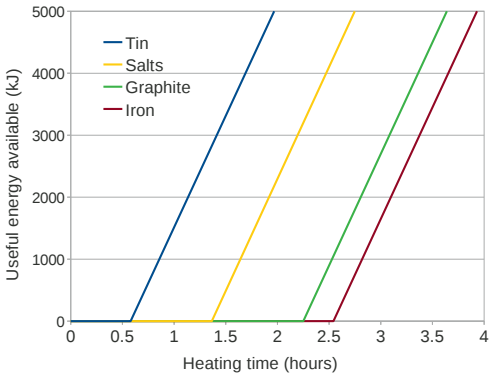

Figure 4: Useful energy available in each storage during the heating, for a heating power of 1 kW, starting at 40°C

6. Interpretation of the results and selection of a storage

Comparing the heat capacities of the five differents materials shows that the latent-heat based systems are more effective than the sensible-heat. This is due to the latent heat which reduces the volume and then the heating time.
However, other parameters must be considered regarding, by importance:

- The chemical stability and the safety (for example: dilatation or vaporization which can increase pressure, chemical reaction between fluids and salts; while iron, carbon and tin are stable)
- The price (tin is very expensive, salts or iron are cheap)
- The heat conductivity (low in salts)
- The weight (a salt storage is light while an iron storage is very heavy)

All these parameters must be considered to choose the best storage regarding the restrictions we have.

7. Conclusion

The potential of the latent heat is huge compare to the sensible heat, especially for a system operational in a precise range of temperatures. It reduces the size of the system and so reduce the heating time before the system is operational. However, others parameters must be considered such as safety, cost, weight or heat conductivity.

References

[1] H. Tabor. A solar cooker for developing countries. *Solar Energy*, 10:153–157, 1966.

[2] N. Nahar. Performance and testing of an improved hot box solar cooker. *Energy conversion and management*, 30:9–16, 1990.

[3] N. Nahar. Performance and testing of a hot box solar cooker. *Energy conversion and management*, 44:1323–1331, 2003.

[4] K. Schwarzer and M.E. Vieira da Silva. Characterisation and design methods of solar cookers. *Solar Energy*, 82:157–163, 2008.

[5] A. Gallagher. A solar fryer. *Solar Energy*, 85:496–505, 2011.

[6] C.W. Foong, O.J. Nydal, and J. Lovseth. Investigation of a small scale double-reflector solar concentrating system with high temperature heat storage. *Applied Thermal Engineering*, 31:1807–1815, 2011.

[7] David V. Ragone. *Thermodynamics of materials and Vol. 1.* Wiley MIT, 1995.

[8] A. Bejan and A. Kraus. *Heat transfer handbook*. Wiley, 2003.

[9] R.M. Muthusivagami, R. Velraj, and R. Sethumadhavan. Solar cooker with and without thermal storage: A review. *Renewable and Sustainable Energy Reviews*, 14:691–701, 2010.

[10] P. Kariuki Nyahoro, Richard R. Johnson, and J. Edwards. Simulated performance of thermal storage in a solar cooker. *Solar Energy*, 59:11–17, 1997.

[11] A. Mawire, M. McPherson, R.R.J. van den Heetkamp, and S.J.P. Mlatho. Simulated performance of storage materials for pebble bed thermal energy storage (tes) systems. *Applied Energy*, 86:1246–1252, 2009.

[12] D. Buddhi and L.K. Sahoo. Solar cooker with latent heat storage: Design and experimental testing. *Energy conversion and management*, 38:493–498, 1997.

[13] H.M.S Hussein, H.H.El-Ghetany, and S.A. Nada. Experimental investigation of novel indirect solar cooker with indoor pcm thermal storage and cooking unit. *Energy conversion and management*, 49:2237–2246, 2002.

[14] A. Sharma, C.R. Chen, V.V.S. Murty, and A. Shukla. Solar cooker with latent heat storage: A review. *Renewable and Sustainable Energy Reviews*, 13:1599–1605, 2009.

B. Influence of solar tracking inaccuracy and sun rays modeling on the efficiency of a small-scale parabolic trough

Maxime Mussard, Ole Jørgen Nydal

To be presented at the ISES Solar World Congress, Cancún, Mexico.
November 2013.
Accepted for publication in Energy Procedia, 2013.

Available online at www.sciencedirect.com

SciVerse ScienceDirect

Energy Procedia 00 (2013) 000–000

Energy Procedia

www.elsevier.com/locate/procedia

2013 ISES Solar World Congress

Influence of solar tracking inaccuracy and sun rays modeling on the efficiency of a small-scale parabolic trough

Maxime Mussard*, Ole Jørgen Nydal

NTNU, Department of Energy and Process Engineering, Kolbjørn Hejes vei 1D, Trondheim 7491, Norway

Abstract

Tracking systems for parabolic troughs are already well designed for industrial processes, but the challenges can be different concerning small-scale low cost systems. Considering cost limitations, some flexibility and error margin on tracking accuracy may be tolerated, due to the imperfections of the parabola or the inaccuracy of the tracking. The objective of this study is to compute the efficiency losses when changing the sun rays incident angles and conclude about the error margin tolerable for a small-scale parabolic trough. Starting from an ideal case, the evolution of the trough efficiency regarding the tracking angle is observed in the plane perpendicular to the axis of a polar mounted trough. A ray tracer is used to simulate the illumination of the absorber. A simplified model for representing the angles of rays from the sun is suggested to take account of all the rays not being parallel.

Selection and/or peer-review under responsibility of ISES

Keywords: sun tracking ; solar angle ; ray tracing

1. Introduction

The accuracy of the tracking of a solar concentrator is often a critical point [1]: a small error can lead to huge losses. For an accurate system, the issue is not critical and considering the rays parallel is a good approximation [2]. Simulations can be also made considering this point and lead to realistic results [3]. This hypothesis is globally admitted while working with a spot of rays coming from the sun, even for solar parabolic troughs [4]. But considering a low-cost solar cooker, the accumulation of small imperfections can also generate significant losses of energy and efficiency. A trough-based system is even more sensible to tracking errors, due to the small size of the image [5]. The rays of the sun are normally considered parallel for computations and ray tracing made in solar energy research [6]; the non-parallel rays gives a high limit for the theoretical possible concentration factor in concentrating systems. However,

* Corresponding author. Tel.: +47 735 93899
E-mail address: maxime.mussard@ntnu.no.

the apparent diameter of the sun gives an angle of about 0.5°. A point of the earth oriented towards the sun can then see rays coming from a cone whose angle is the apparent diameter of the sun [5, 7]. The consequences of this approximation are in general negligible; but in some particular case, significant errors can be done.

2. Preliminary work

Considering a low-cost small scale solar parabolic trough, the considerations of perfect reflection of the rays is not suitable. Indeed, the inaccuracy of the parabola is then non negligible, and the tracking could sometimes be not precise enough to compensate these small defaults. The consequences of a tracking error, even below 1 °, can become a real challenge. Considering the rays of the sun parallel will lead, in certain cases, to different results than considering them coming from slightly different angles. The case study is a parabolic trough, 1x1.05m size, with a 2 cm-diameter pipe (Figure 1).

Fig. 1. Small-scale low-cost parabolic trough with heat storage for cooking purposes

3. Ideal case

Starting from a parabolic trough, size 1x1.05 meter (Fig. 2), with an absorbing pipe of 0.5 cm diameter on the focal line of the trough, we can compute the path of the rays using a ray tracer. The simulation is done considering the trough perfectly oriented and the rays parallels. All the rays are then focusing on the focal line.

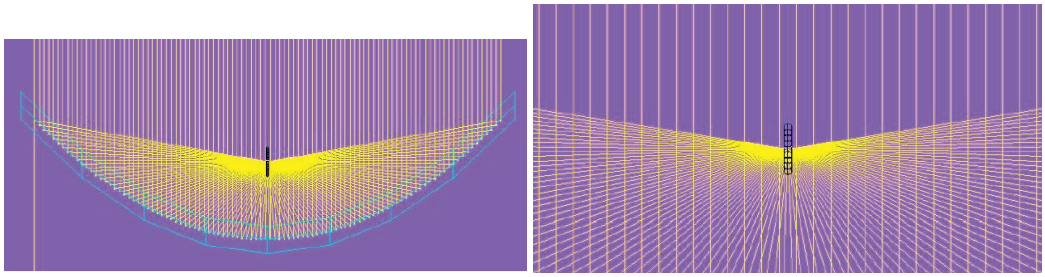

Fig. 2. Ray tracing for a 1.05-m large parabolic trough, 0.5 cm diameter absorber, 0° inclination

For an angle of 0.5°, around half of the rays do not reach the absorber anymore (Fig. 3).

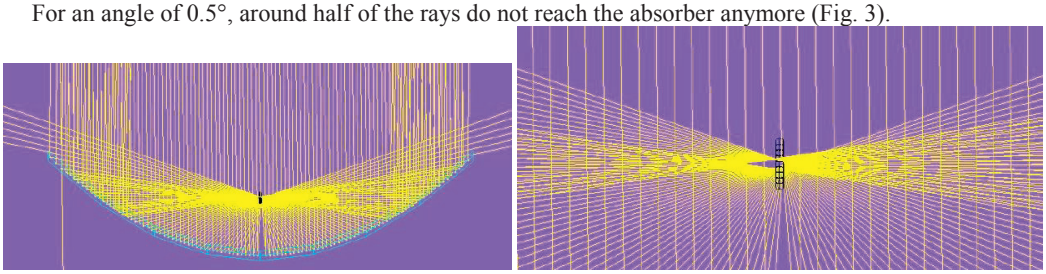

Fig. 2. Ray tracing for a 1.05-m large parabolic trough, 0.5 cm diameter absorber, 0.5° inclination

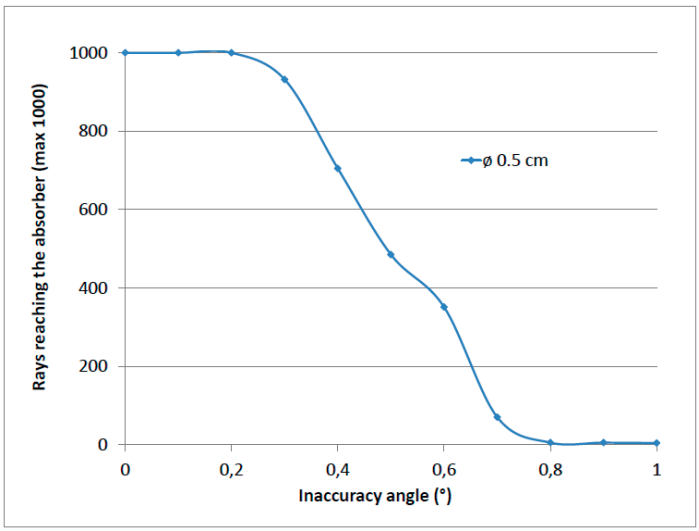

Fig. 4. Rays reaching the absorber as function of the tracking error (from 0 to 1°)

By considering then a tracking error, the number of rays hitting the trough is decreasing. Fig. 4 shows the losses as the tracking angle deviates up to 1°. Fig. 4 shows the efficiency of the trough (proportional to the number of rays reaching the absorber) regarding the tracking error, considering all rays parallels.

4. Modeling of the sun

In the ideal case, 1000 rays were considered coming all parallel. The computation model gives then precise results for the ideal case. For the next computations, 1000 rays are considered coming from 3 different angles, to take into account the solar angle; the intensity chosen for each angle is then weighted by a coefficient to fit with the solar angle. For the graphic representations, only 100 rays are represented.

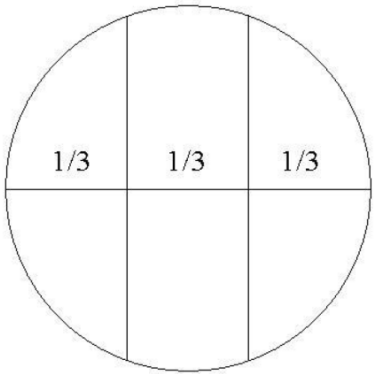

Fig. 5. Discretization of the dish

4.1. Average absolute angle of the rays from the sun

Considering the sun as a dish, the distribution of the rays of the sun coming in a same plane is maximal at the center and null at the two extreme points. The weight of each slice of the dish is proportional to the area covered by that slice. If three slices are considered instead of one, the objective is then to distribute the rays so that we get a model as representative as possible.

The origin of the angle is the middle of the sun. The intensity of the sun regarding the angle is described by the equation of the quarter of a circle, considering 0.53°of apparent angle, so 0.265° for the half angle, called α (α is then the half-diameter of the circle):

$$f(x) = \sqrt{1 - (\frac{x}{\alpha})^2} \tag{1}$$

where 1 is the maximum intensity, reached at the middle of the dish (x = 0).

If we consider that the average angle of the rays of the sun is 0°, and the maximum +- 0.265 °, then the averaged absolute value of the angles of the rays is the ratio between the intensity weighted by the angle and the intensity, both integrated between 0 and the half-angle:

$$\frac{\int_0^\alpha x\sqrt{1-(\frac{x}{\alpha})^2}\,\mathrm{d}x}{\int_0^\alpha \sqrt{1-(\frac{x}{\alpha})^2}\,\mathrm{d}x} \simeq 0.112 \tag{2}$$

The rays of the sun are seen by an average angle of 0.112° (in absolute value).

4.2. Distribution of the rays

Instead of drawing all the rays parallels, they are then distributed by spots. The sun is then sliced in three parts, each part covers one third of the total diameter. To simplify, the calculations are done on the upper right quarter of the dish (Fig. 6).

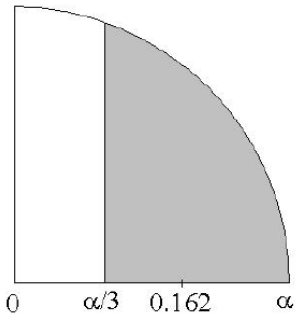

Fig. 6. Upper right quarter of the dish

To calculate the average angle for the right third of the dish, the same formula than previously is used:

$$\frac{\int_{\alpha/3}^{\alpha} x\sqrt{1-(\frac{x}{\alpha})^2}\,\mathrm{d}x}{\int_{\alpha/3}^{\alpha} \sqrt{1-(\frac{x}{\alpha})^2}\,\mathrm{d}x} \simeq 0.162 \tag{3}$$

The rays leaving the right third of the sun have then an average angle of 0.162°. It is easy to guess that they represent less than the third of the rays. Dividing the area of the right third by the total area of the circle (considering a full dish starting from the formula of an upper quarter), we get then:

$$\frac{2\int_{\alpha/3}^{\alpha} \sqrt{1-(\frac{x}{\alpha})^2}\,\mathrm{d}x}{4\int_{0}^{\alpha} \sqrt{1-(\frac{x}{\alpha})^2}\,\mathrm{d}x} \simeq 0.29 \tag{4}$$

The right third represents then around 29% of the rays; by symmetry, the left third represents 29% as well.

The central third represents then 42% of the rays. This weighting will be used in the next computations. We got finally: 29% of the rays seen by an angle of -0.162° from the center of the sun, 42% seen by an angle of 0°, and 29% seen by an angle of +0.162° (Fig. 7).

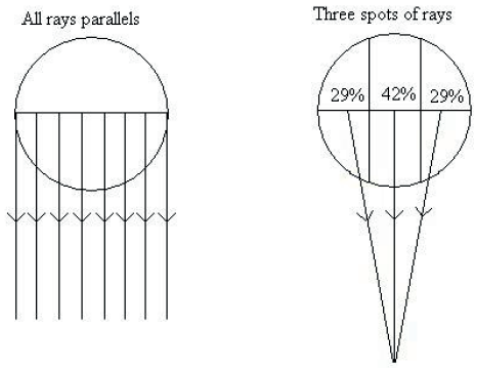

Fig. 7. Comparison of the 2 models of the sun

5. Correction of the ideal case considering three spots of rays

Applying this model of the sun to the original model gives the following result. We can see on the Figure 8 the difference between the first model considering all rays parallels, and the second one considering some of the incoming rays with an angle of +/- 0.162°.

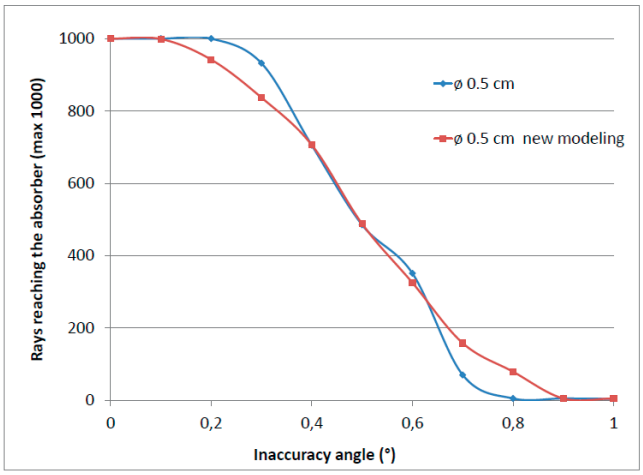

Fig. 8. Rays reaching the absorber regarding the tracking error: comparison of the 2 models

This difference can be observed by comparing the behavior of rays coming from different angles. For example, for an average incoming angle of 0.3°, the efficiency is then 93 % if all the rays are considered parallel; but with the new model, it is around 84 %, due to the weight of the rays coming from an angle of 0.3°+0.162° in this case.

Now, considering the two other spots: 100% of the rays coming from an angle of 0.3° - 0.162° reach the absorber; but only 54% of the rays coming from an angle of 0.3°+0.162°.

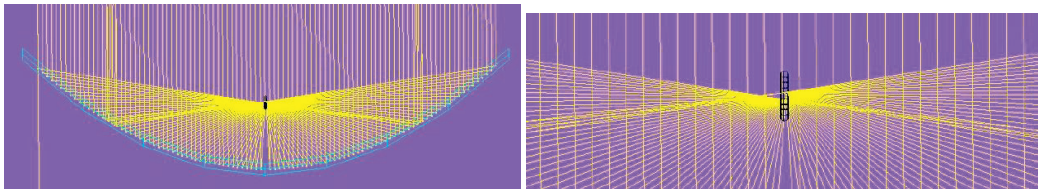

Fig. 9. Ray tracing for a 1.05-m large parabolic trough, 0.5cm diameter absorber, 0.3° inclination

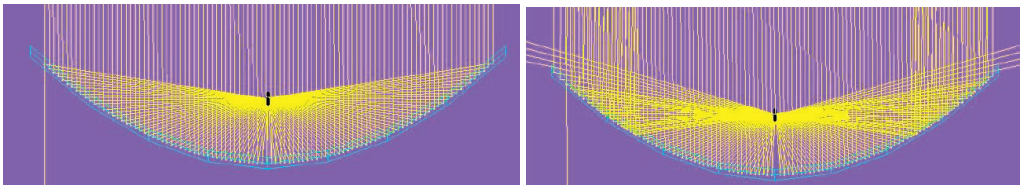

Fig. 10. Ray tracing for a 1.05-m large parabolic trough, 0.5cm diameter absorber, 0.3° - (a) and + (b) 0.162° inclination

6. Influence of the diameter of the absorber

Increasing the diameter of the absorber allows more freedom concerning the accuracy of the tracking. By taking a 2 cm-diameter absorber instead of 0.5 cm, the system will collect more rays for a given angle. For example, for the rays coming with a 0.8° inclination, all the rays join the absorber.

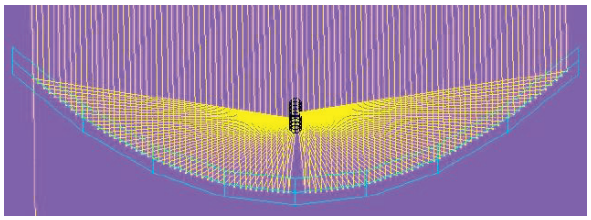

Fig. 11. Ray tracing for a 1.05-m large parabolic trough, 2 cm diameter absorber, 0.8° inclination

It is possible then to compute the efficiencies for different diameters of the absorber.

The difference between the two models gets smaller when the diameter of the pipe increases.

With a small pipe diameter, the difference can be up to 9 % (for a 0.3° angle). For the 2 cm-diameter pipe, the difference is not higher than 2 % for an angle of 1.1°. The data for pipes of 0.5, 1 and 2 cm diameter are then plotted (Fig. 12).

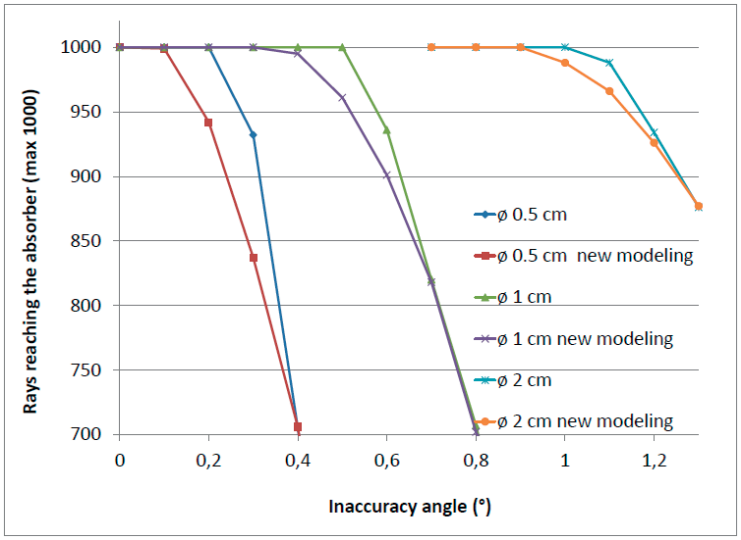

Fig. 12. Rays reaching the absorber regarding the tracking error: comparison of the 2 models for 3 different pipe diameters

7. Conclusion

The tracking must be precise concerning a parabolic trough. Increasing the diameter of the absorber is a solution to tolerate more tracking inaccuracy. Considering the rays of the sun parallels is often quite realistic, but in certain cases the precision of this modeling is not excellent anymore. Close to the critical angles, an error of 9 % concerning the efficiency can be made by considering the rays parallels. A simplified model which takes into account the apparent angle of the sun can provide an estimation of this imprecision.

References

[1] Zhang J, Sun F, Zhang X, Guo M, Wang Z. Accurate altitude azimuth tracking angle formulas for a heliostat with mirrorpivot offset and other fixed geometrical errors. *Solar Energy* 2011;**85**:1091–1100.

[2] Abu-Malouh R, Muslih I, Abdallah S. Design, construction and operation of spherical solar cooker with automatic sun tracking system. *Energy Conversion and Management* 2011;**52**:615–620.

[3] Sellami N, Mallick T, McNeil D. Optical characterisation of a 3-D static solar concentrator. *Energy Conversion and Management* 2012;**64**:579–586.

[4] Dai J, Kang H, Zheng H, Tao T. Light tracing analysis of a new kind of trough solar concentrator. *Energy Conversion and Management* 2011;**52**:2373–2377.

[5] Mo S, Chen Z, Jiang S, Hu P. Optical modeling for a two-stage parabolic trough concentrating photovoltaic/thermal system using spectral beam splitting technology. *Solar Energy Materials and Solar Cells* 2010;**85**:1686–1696.

[6] Yu W, Zhang H, Wang Z, Wei X, Lu Z. Tracking and ray tracing equations for the target-aligned heliostat for solar tower power plants. Mo S, Chen Z, Jiang S, Hu P. Optical modeling for a two-stage parabolic trough concentrating photovoltaic/thermal system using spectral beam splitting technology. *Renewable Energy* 2011;**36**:2687–2693.

[7] Riveros H. Graphical analysis of sun concentrating collectors. *Solar Energy 1985*;**36**:313–322.

C. Heating of an oil-based heat storage with a low-cost small-scale solar parabolic trough

Maxime Mussard, Erwan Vaujany, Ole Jørgen Nydal

Proceedings of the EuroSun2012 - ISES Europe Solar Conference, Rijeka, Croatia. September 2012.

Heating of an oil-based heat storage with a low-cost small-scale solar parabolic trough

Maxime Mussard, Erwan Vaujany, Ole Jørgen Nydal

NTNU, Department of Energy and Process Engineering, Kolbjørn hejes vei 1D, Trondheim, Norway

Abstract

Experimental results regarding the charging of a heat storage with a small-scale low-cost parabolic trough are described. The main objective is to study a system storing the heat collected during the day for use as a heat source for cooking, drying or for other applications at times without sunshine. The system is liquid-based: the collector concentrates the energy on the receiver so that the fluid inside the receiver is heated and can carry the energy to the storage. The loop connecting the collector and the storage is filled with a thermal fluid (Syltherm 800) which circulates by the self-circulation principle. A mechanical clockwork orientates the system to track the sun. The experiments are run during sunny days for limited charging periods (around 2 hours). A simulation model is then build based on these results to extrapolate the behaviour of the system. Temperature measurements are compared with a dynamic model for self-circulating systems.

Keywords: heat storage, solar parabolic trough, oil-based storage, thermosyphon

1. Introduction

Solar cooking has been promoted since many years to reduce the use of non-renewable energies (charcoal, wood, fuel) in sunny areas. However, when the sun is too weak (evening, night, cloudy day), the system needs a backup and/or an efficient heat storage. The most common way of heating is the direct heating. Solar cooking by direct illumination is generally efficient enough, ever with a parabola[1][2] or a box cooker[2]: the energy is instantaneously transmitted to the application; the losses are quite high but the heating time reasonably low. Charging a heat storage by direct illumination with a concentrator is an option, the energy of the storage can then be used for cooking[3]. Some studies have been done on charging a heat storage with a flat collector and a thermosyphon loop[4][2] or a concentrating system[2][5]. The objective here is to test a small-scale low cost parabolic trough charging a heat storage for cooking purposes. The technology of the parabolic trough has been developed since many years, the main part of the solar power plants is now based on this concept. The system works with the thermosyphon principle; using a parabolic trough increases the concentration ratio compare to the flat collector[6].
The system is developed to be used in a rural African setting, so the simplicity and affordability of the system are important parameters.

Email address: maxime.mussard@ntnu.no (Maxime Mussard, Erwan Vaujany, Ole Jørgen Nydal)

2. Objectives

Reaching a temperature above 200°C in the storage is necessary to have a system able to cook and fry food in reasonable time; the main objective of the project is to get a system able to fry Injera bread (a typical Ethiopian bread) in an efficient way and to keep the quality of the bread[1]. The main objective of this article is to describe the results of the experiments concerning the charging of a heat storage with a small-scale low-cost solar parabolic trough. The storage is filled with avocado oil, we can then study the behaviour of the system for heat extraction into the storage. The avocado oil has been chosen due to its high heat tolerance[7]. To study the seld-circulation properties of the Syltherm 800, a reduced amount of oil is used in the storage. The system then has a low sensible heat and the temperature will increase quickly.

3. Description of the system

The system is based on a self-circulating loop starting at the absorber. A 1-meter long copper tube is then linked with a 50 cm long stainless-steel flexible pipe. This pipe is then connected to a copper spiral running into the storage. At the outlet of the storage, the spiral is connected to the inlet of the absorber with a 50 cm tube and a 1.90 meter long flexible pipe. The loop is open to the atmosphere and has an expansion tank.
The system is insulated with aerogel, except the absorber which is not insulated at all. Aluminium foils are used to reduce the radiation losses.
The reflector is covered with a reflective film, the trough is made of wood pieces and the tracking is a Scheffler-based clockwork[8].
The loop is filled with Syltherm 800, the total volume is around 0.8 liter.
Apart from the Syltherm and the aerogel, the others materials are easily available in a rural African setting. Others oils can be investigated, and it is possible to use glasswool as insulation.
The Figure 1 shows a schematic view of the loop, the inside diameters and length of each part are precised here.

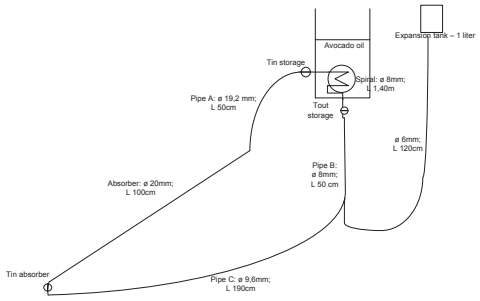

Figure 1: Oil-based storage coupled with a self-circulated loop

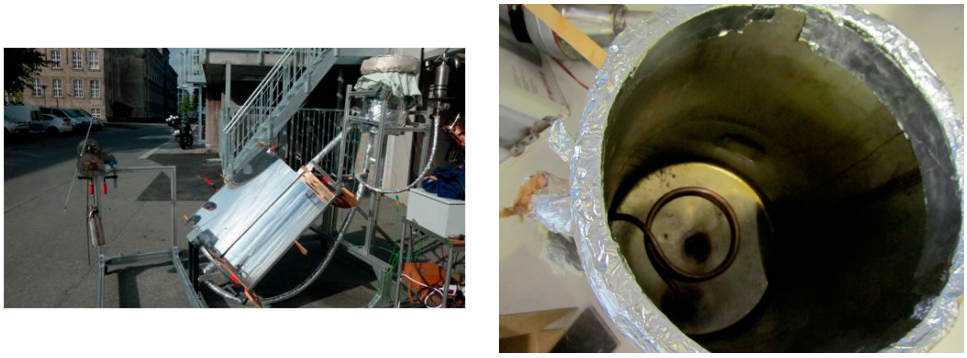

Figure 2: Oil-based storage coupled with a self-circulated loop - system in operation and view of the spiral

4. Experiments: Oil-based storage

The experiments took place in Trondheim (63°North) during sunny days. The trough is then much more inclined than it should be in Africa. The Figure 2 shows the system in operation, and the spiral in the storage (notice the insulation layer around the storage).
The storage contains 8 kilogramms of avocado oil. The results obtained during a 2 hours sun time are plotted on Figure 3. The storage is heated up to 105°C within this short heating time.

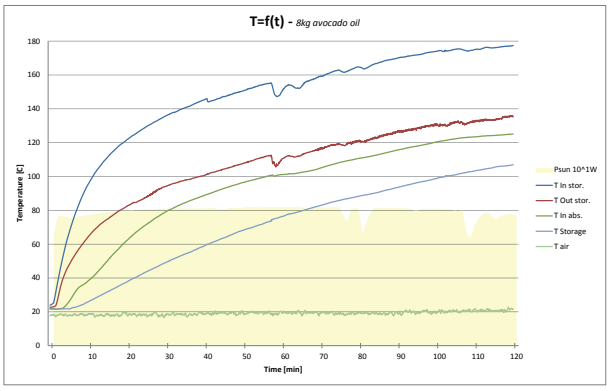

Figure 3: Heating of an oil-based heat storage under sunny conditions

5. Simulation of the oil-based storage

5.1. Parameters of the simulation of the oil-based storage

Based on these results, a model is then programmed using a spreadsheet. The loop is discretized in 73 slices of 10 cm each. The simulation computes the temperatures, velocities and physical properties every second. The following datas are used:

Absorber diameter: $D_{abs} = 20$ mm; length: $L_{abs} = 1$ m
Pipe A: $D_A = 19.2$ mm, $L_A = 0.5$ m
Pipe B: $D_B = 8$ mm, $L_B = 0.5$ m
Pipe C: $D_C = 9{,}6$ mm, $L_C = 1.9$ m; where: D_X is the diameter and L_X is the length of the pipe X
Spiral: $D_{sp} = 8$ mm, $L_{sp} = 1.4$ m; where D_{sp} is the diameter and L_X the length of the spiral
2 elbows: $L/D = 100$, Pressure drop parameter due to elbow friction
$g = 9.81$ m/s^2, Gravitation constant
$h = 1.2$ m, Height difference between the beginning of the absorber and the beginning of the spiral
$h_{spiral-storage} = 110$ W/m2.K, Heat transfer coefficient between the spiral and the oil of the storage
$h_{abs} = 15$ W/m^2.K, Heat transfer coefficient between the absorber and the atmosphere
$M = 10$ kgs, Mass of the storage, container included
$C_{p-storage} = 1500$ J/K.kg, Average heat capacity of the storage, container included
$T_{out} = T_{start} = 293$ K; where T_{out} is the outdoor temperature and T_{start} the starting temperature
$C_{pvol-syltherm} = 1500$ J/K.l, Volumetric heat capacity of Syltherm 800, approx. constant with T
$e_{storage} = e_{pipeA} = 1.2$ cm
$e_{pipeB} = e_{pipeC} = 0.8$ cm; where $e_{storage}$ is the thickness of the insulation of the storage and e_{pipeX} the thickness of the insulation of the pipe X
$P_{losses-stg} = 0.8$ W/K, Thermal losses of the storage (value computed during the cooling of the system)
$P_{losses-A} = 0.1$ W/K
$P_{losses-B} = P_{losses-C} = 0.035$ W/K; where $P_{losses-X}$ are the thermal losses of the pipe X
$\epsilon = 0.03$, Emissivity of the absorber
$\lambda_{agl} = 0.02$ W/m.K, Heat conductivity of the aerogel
$r = 0.7$, Reflectivity of the collector
$a = 0.85$, Absorption coefficient of the absorber
$P_{sol} = 800$ W/m^2, Solar constant
$A = 1.05$ m^2, Area of the collector
Notice that M represents the mass of oil in the storage plus the virtual mass of oil corresponding to the sensible heat of the walls of the storage.

5.2. Step 0

The system starts at $t = 0$ at 293 K. The velocities and mass flows are equal to 0. The viscosity of the oil is corresponding to the viscosity of the average temperature of the system (a formula based on the offical datasheet of the Syltherm 800 is used). The atmosphere is at 293 K.

5.3. Step 1

At $t = 1$ *sec* the solar energy is applied as heat source into the absorber. According to the experimental data, we got a solar radiation of around 800 W/m^2. Considering around 30 % of

lossed due to the bad quality of the mirror and the tracking inaccuracy; and an absorption coefficient of 0.85, we then estimate a power of around 475 W absorbed by the Syltherm in the absorber (around 59% of the energy reaching orginally the collector). The absorber is discretized by 10 slices of 10 cm each, so each of the 10 slices gets 10% of 475 Watts. The temperature of the syltherm in the absorber increases, the rest of the loop is still at 293 K. A difference of oil density is then generated and will start the thermosyphon.

5.3.1. Single-phase gravity driven flow

The difference of density between the upward-flow part (absorber, pipe A) and the downward-flow part (spiral, pipe B and pipe C) drives the flow. Considering the flow as laminar, we have from the Darcy-Weisbach equation:

$$\frac{\Delta P}{L} = \frac{\Delta \rho g h}{L} = \lambda \rho \frac{U^2}{2} \frac{1}{D}$$

Where ρ is the density of the fluid, U the velocity and ΔP the pressure drop; and λ the Darcy friction factor for laminar flows:

$$\lambda = \frac{64}{Re} = \frac{64\mu}{\rho D U}$$

where Re is the Reynolds number and μ the dynamic viscosity; and we have the volume flow M_v. We approximate μ and ρ homogeneous along the loop for the friction calculation, using the temperatures computes previously (with the method described at the step 0). The equation applied to our case is then:

$$M_v = \frac{U \pi D^2}{4} = \frac{\rho g h D^4 \pi . \Delta \rho}{128 \mu L}$$

$\Delta\rho$ is computed with the difference of the average temperatures of the upward and the downward parts (A linerar equation is used to compute the density depending of the temperature). Knowing the M_v, this gives the velocity inside each of the pipes and tubes.

5.3.2. Energy equation

The energy equation of the full system is then:

$$P_{sys} = raAP_{sol} - h_{abs}(T_{abs} - T_{out}) - \sigma \epsilon L_{abs}(T_{abs}^4 - T_{out}^4) - \Sigma P_{losses-X}(T_X - T_{out}) - P_{losses-str}(T_{str} - T_{out})$$

where P_{sys} is the net energy stored in the system per second and σ the Stefan-Boltzmann constant.

5.4. Step 2

The step 2 ($t = 2\ sec$) follows the step 1 for all the parameters. In addition, the Syltherm starts flowing and the storage is heated depending on the temperature of the fluid in the spiral. First, the temperature of the storage is calculated related to the temperature of the fluid of the spiral at the step 1, and losses by conduction are applied to it. Notice that the temperature is still at 293 K both in the spiral and in the storage, the oil didn't start moving at this point.
Using the velocities computed at the step 1, we compute then new temperatures for each of the slice of the system, considering their temperature at the step 1 and the temperature of the previous slice at the step 1, weighted with the velocity computed in 1. The losses by conduction

and the heating of the pipe and insulation are applied to the pipes A, B and C; losses by convection to the storage are applied to the spiral. New viscosity and velocities are then compute based on the new temperatures.

5.5. Step n

At $t = n$ sec, we follow the computation done at the step 2, using the step n-1 instead of 1.

6. Exploitation of the model

6.1. Comparison of the model with the experiments

The storage contains 8 kilogramms of avocado oil. The results obtained during a 2 hours sun time are plotted on Figure 4. The simulation fits with the experimental results, except for the beginning (difficulty to simulate precisely the heating of the pipe and insulation).

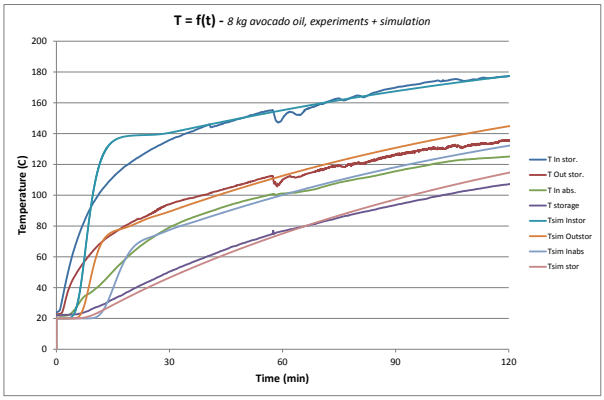

Figure 4: Comparison between experiment and simulation of the heating of an oil-based heat storage

6.2. Improvement of the system - simulation of the oil-based storage

First, a thin layer of insulation was used, and the insulation pillow was not totally sealed. By improving the system, it should be possible to inscrease the insulation by a factor 10.
Secondly, the tracking system and the reflective surface was not optimized for the system. By improving these 2 parameters as well, it is reasonable to expect an improvement of 15% of the heat collection. Simulating during 8 hours leads to a storage temperature of 250°(Figure 5).

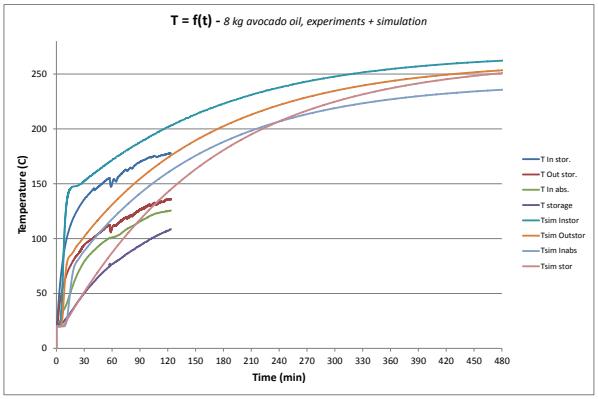

Figure 5: Simulation with improved insulation and heat collection of the heating of an oil-based heat storage

Finally, the model simulates an evacuated tube absorber, which divides the convective heat losses by 10[6]. The temperature in the storage can then theoritically reaches 350°C (Figure 6). Notice that the Sylltherm 800 and the avocado oil are not stable at these temperatures.

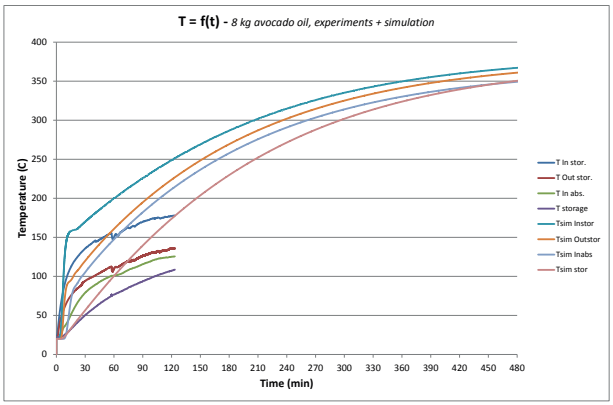

Figure 6: Heating simulation with improved insulation, heat collection and evacuated tube absorber

7. Thermal efficiencies of the system depending of the improvements

In Table 1, the ratio (in %) between the total amount of energy reaching the collector and the energy stored at a defined time are computed.
The efficiency decreases when the temperature of the full system increases, which is due to higher heat losses. Considering that the system starts from 20°C, the difference between the efficiencies are large depending on temperature and energy stored.

System improvements	Eff. after 2 hrs	After 8 hrs
Basic system	24.5	9.9
+ improved insulation	27.9	13.3
+ improved collection	31.8	15.0
+ evacuated absorber	40.1	21.5

Table 1: Efficiency of the system depending of time and improvements

8. Conclusion

The heat collection with a parabolic trough is promising for storing heat above 200°C. For this, an optimization of the current system is necessary. Improved reflector performance and use of evacuated tube absorber can increase the price. A balance between the energy gain and the cost will lead to an optimal system.

References

[1] A. Gallagher. A solar fryer. *Solar Energy*, 85:496–505, 2011.

[2] S. Kothari N.L. Panwar, S.C. Kaushik. State of the art of solar cooking: An overview. *Renewable and Sustainable Energy Reviews*, 16:3776–3785, 2012.

[3] O.J. Nydal C.W. Foong, J. Loevseth. Investigation of a small scale double-reflector solar concentrating system with high temperature heat storage. *Applied thermal engineering*, 31:1807–1815, 2011.

[4] M.E. Vieira da Silva K. Schwarzer. Characterisation and design methods of solar cookers. *Solar Energy*, 82:157–163, 2008.

[5] Hensel W. Scheffler A. Munir, O. Design principle and calculations of a scheffler fixed focus concentrator for medium temperature applications. *Solar Energy*, 84:1490–1502, 2010.

[6] W.A. Beckman J.A. Duffie. *Solar Engineering of Thermal Processes*. Wiley MIT, 1995.

[7] Diana Ansorena I. Astiasarn I. Berasategi, Blanca Barriuso. Stability of avocadooil during heating: Comparative study to olive oil. *Food Chemistry*, 132:439–446, 2012.

[8] V. Sardeshpande. Investigation of a small scale double-reflector solar concentrating system with high temperature heat storage. *Energy for Sustainable Development*, Under press, 2012.

D. Comparison of oil and aluminum-based heat storage charged with a small-scale solar parabolic trough

Maxime Mussard, Ole Jørgen Nydal

Applied Thermal Engineering, Volume 58, Issues 1-2, pp. 146-154, 2013.

Is not included due to copyright

E. Charging of a heat storage coupled with a low-cost small-scale parabolic trough for cooking purposes

Maxime Mussard, Ole Jørgen Nydal

Solar Energy, Volume 95, pp. 144-154, 2013.

Is not included due to copyright

F. Experimental study of solar cooking using heat storage in comparison with direct heating

Maxime Mussard, Alexandre Gueno, Ole Jørgen Nydal

Accepted for publication in Solar Energy, 2013.

Experimental study of solar cooking using heat storage in comparison with direct heating

Maxime Mussard, Alexandre Gueno, Ole Jørgen Nydal

Department of Energy and Process Engineering, Norwegian University of Science and Technology
Kolbjørn Hejes vei 1D, Trondheim, Norway

Abstract

The paper presents a comparative experimental study of two solar cookers. The first is the widespread SK14 cooker; the second is a prototype of a solar concentrator (parabolic trough) using a storage unit. The SK14 is a direct solar cooker where the cooking pot is placed on the focal point of a parabolic dish; in the trough system heat is transported from an absorber to a storage unit by means of a self-circulation loop filled with thermal oil. Cooking takes place directly on the top of the storage. Cooking experiments are conducted to compare the performance of these two methods of heat extraction. Both boiling and frying are tested to estimate the cooking efficiency of the heat storage system. Following these experiments, simulations are conducted to optimize and improve the system. Cooking on a heat storage with optimized surface contact is proved to be competitive with standard solar cookers or other cooking devices.

Keywords: heat storage, heat extraction, solar cooking

1. Introduction

To overcome the demand for energy in countries where a large part of the population lives without electricity, solar cookers have been designed and developed in numerous projects, with concentrative mirrors[1], flat collectors[2] or box cookers[3, 4].

These solar cookers use the substantial amount of energy available directly from the sun instead of non-renewable energy sources (charcoal, wood from local forests, fuel). There is a large variety of solar cookers which focus the sunlight directly on the cooking pot. Thus their use is limited to sunny days in warm areas. To overcome this problem and improve the development of solar cookers, a heat storage unit is necessary. It can then be theoretically possible to cook during the night or on a cloudy day. Many options have been investigated, such as charging the heat storage by direct heating with a concentrator[5]; with a flat collector and a thermosyphon loop[2, 6], a concentrator system[6, 7, 8, 9]; or with a Scheffler reflector[10]. Charging with evacuated tubes and storage with phase-change materials (PCM) at 120°C have been tested[11], as well as performance evaluation of a heat storage[12], discharging simulation[13], endurance test for PCM in a storage[14], comparison of heat storage[15] and exergy analysis[16].

Email address: maxime.mussard@ntnu.no (Maxime Mussard, Alexandre Gueno, Ole Jørgen Nydal)

When considering a heat storage system, the heat extraction to the application is a major issue. Modifying the shape of the vessel is an option[17], as is optimizing the vessel area in contact with heat[18] or relying on latent heat[19]. These solutions necessitate a change in cooking habits, so cooking on a simple hot plate is worth investigating. The SK14 is a widespread direct solar cooker[20] and a comparison between its performance and that of a heat storage system is discussed in this paper.

Nomenclature

α_p	Absorption coefficient
β_p	Corrector coefficient
ΔT	Difference between the ambient and the water temperatures (°C)
ϵ	Emissivity of the pot
γ_p	Reflection coefficient
λ	Air thermal conductivity (W/m.K)
λ_m	Thermal conductivity of the meat (W/m.K)
λ_{olive}	Olive oil thermal conductivity (W/m.K)
ϕ	Energy flux received from the sun (W/m^2)
ϕ_c	Losses by convection (W)
ϕ_i	Losses through the insulation (W)
ϕ_r	Losses by radiation (W)
ϕ_{meat}	Energy transmitted to the meat (W)
ρ_m	Density of the meat (kg/m^3)
ρ_o	Density of Duratherm 630 oil (kg/m^3)
ρ_{olive}	Density of olive oil (kg/m^3)
A_m	Bottom area of the meat (m^2)
A_{pan}	Bottom area of the pot (m^2)
C_p	Heat capacity of water (kJ/kg.K)
C_{p_m}	Heat capacity of the meat (kJ/kg.K)
C_{p_o}	Heat capacity of Duratherm 630 oil (kJ/kg.K)
C_{p_s}	Heat capacity of the solar salts (kJ/kg.K)

$C_{p_{olive}}$ Heat capacity of olive oil (kJ/kg.K)

d Diameter of the pan (m)

d_m Diameter of the piece of meat (m)

e Thickness of the olive oil layer (between meat and pot)(m)

h Losses by convection (W)

h_m Thickness of the piece of meat (m)

L Insulation thickness (m)

m Mass of water (kg)

m_{stor} Mass of the storage unit (kg)

R_{ext} External radius of insulation (m)

R_{int} Internal radius of insulation (m)

R_{th_p} Thermal resistance of the pan (K/W)

S Surface of the SK14 receiving solar radiation (m^2)

S_{pan} Surface of the wall of the pan (m^2)

T_a Ambient temperature (°C)

T_w Water temperature (°C)

T_{meat} Temperature of the meat (°C)

T_{plate} Temperature of the storage plate (°C)

$T_{storage}$ Temperature of the storage unit (°C)

v Wind speed average (m/s)

z Height of the pan (m)

2. Objectives

The two systems are designed to be used for multipurpose applications, but the main goal for both is to give enough energy to cook in a reasonable time. The objective here is then to compare these two systems during cooking and conclude about the efficiency of cooking using the heat storage system.

The SK14 system does not need any charging, the cooking vessel is positioned directly on the focal point of the parabola. On the other hand, the heat storage system needs several hours of sun to be charged due to its high operating temperature. The storage is based on the latent heat of nitrate salt, which melt at about 220°C. Once this temperature is reached, the user has to simply put a vessel on top of the storage unit to cook.

By trying to boil 1 liter of water in the same pot with both systems, it is possible to get a first approximation of the relative efficiency of the two cookers, we can then conclude about the technical competitiveness of the heat storage-based system.

The first objective is then to compare the time required to boil 1 liter of water initially at ambient temperature, in optimal conditions, for both systems. A frying test and some simulations are then developed to detail the performance of the heat storage system.

3. Experimental setup

The same pot is used in each experiment. It is made of steel with a thickness of 5 mm at the bottom. The temperature of water is recorded with a thermocouple placed in the middle of the pot.

- The SK14 is tested during a sunny, calm day (average insolation: 850 W/m^2) while ensuring that the parabola remains oriented towards the sun. The data recording starts when the vessel is placed on the cooking spot.
- The absorber of the heat storage-based system is heated with an electrical wire until the temperature reaches 220°C in the storage unit. The data recording starts when the vessel is placed on the top of the storage unit. Previous experiments shows that the time required with the sun is almost 5 hours[9], the storage can then be fully charged using solar energy (efficiency of about 20%, starting from ambient temperature to full melting of the salts). For practical and meteorological reasons, electricity is used here to charge the storage.

3.1. Features of the SK14 system

The SK14 is a solar cooker developed by the Foreign Aid Group Solar Cooker ot the State Technical College Altoetting e.V in Germany (Figure 1), the system is a parabola made with reflective strips, its diameter is 140 centimeters[20]. The parabola is held by a structure which allows rotation to follow the sun. A holder is placed so that the vessel is exactly at the focal point. A special pot painted black is provided with the system; but in order to compare our two systems in conditions that are as similar as possible, a standard steel pot was tested. The performance of the SK14 will be then lower than with a black pot.

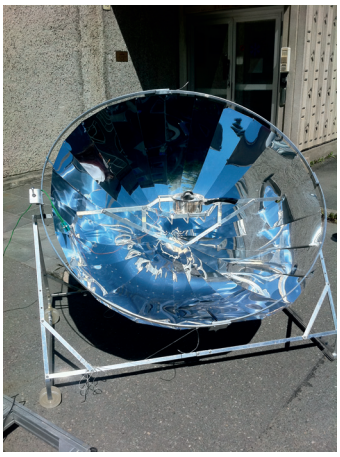

Figure 1: SK14 system

3.2. Features of the heat storage-based system

This prototype is a solar concentrator with a heat storage unit. A closed loop self circulating oil system transfers the heat from an absorber to a storage unit[9]. The absorber (part of the loop) is a copper tube, 1 meter long and 22 mm diameter, painted black. The energy from the sun is focused on the absorber by a parabolic trough. The collector aperture is 1 m^2 and the focal length 20 cm. The oil used was the Duratherm 630. Its thermal properties at 25°C are[21]:
Heat capacity: $C_{p_o} = 1.933$ kJ/kg.K
Density: $\rho_o = 833$ kg/m^3

The storage unit is a steel cylinder with a diameter of 202 mm, insulated with 8 cm of Pyrogel. It is full of oil and closed with a 1 cm-thick lid made of aluminum; this lid has 8 tubes containing a $NaNO_3 - KNO_3$ binary mixture (called melting salts). The aim of putting these salts in is to recover the latent heat[9], knowing that their melting temperature is around 210-220°C.
The following gives the formulas and values of the heat capacity, latent heat included (T in K, C_p in kJ/kg.K)[5]:

$$C_{p_s} = \begin{cases} 0.75 & \text{if } T < 383K \\ 4.1 & \text{if } 378 \leq T \leq 388K \\ 1.4 & \text{if } 388 < T < 488K \\ 12 & \text{if } 488 \leq T \leq 498K \\ 1.6 & \text{if } T > 498K \end{cases}$$

4. Experimental results

4.1. Comparison of cooking efficiency

Heat extraction performance testing of these two systems was conducted in Trondheim, Norway. During each test, the same pan made of inox was filled with 1 liter of water, closed by a lid. Concerning the SK14, the experiment was conducted on 25 June 2012; the average insolation during

Figure 2: Heat storage-based system with parabolic trough

the experiment was around 850 W/m^2 and the ambient temperature 23°C. The solar radiation was measured on a continuing basis at NTNU. For the test of the heat storage system, the experiment was run indoors, the water temperature was initially around 22°C. The storage was initially at 220°C. The water for the SK14 test was originally at 12°C while for the heat storage it was 23°C, only the results from 23°C are then displayed.

On Figure 3, we can see the evolution of the water temperature during the boiling test in both experiments.

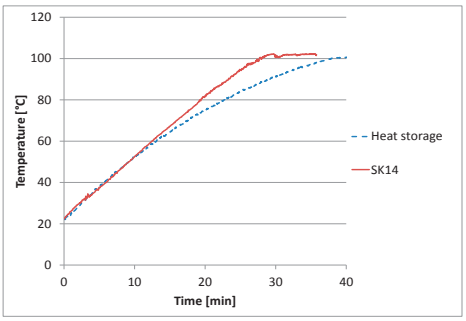

Figure 3: Evolution of the water temperature during a boiling test - SK14 and heat storage-based system

The evolution of the water temperature is linear for the SK14 due to the constant energy flux[22]

while the water temperature increase for the heat storage system slows down when reaching higher temperatures due to the (almost) constant temperature (Cf. Figure 12) in the storage[22].

To reach the boiling point for water, the SK14 system needed 27 min (from 23°C), and 38 min for the heat storage unit. Thus, boiling water with the SK14 seems to be more efficient than the heat storage unit. Further improvements are expected concerning the heat storage system, especially by improving the contact between the pan and the storage: the cylinders containing the solar salts decrease the surface of contact; and the aluminum lid of the storage is not perfectly flat. Another experiment was run to check this hypothesis.

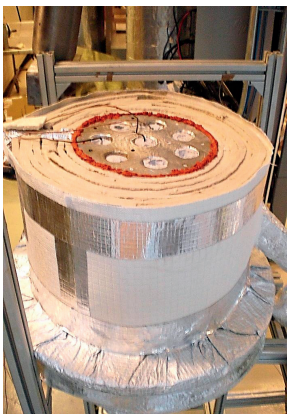

Figure 4: View of the top of the storage: aluminum lid and cylinders containing the salts

4.2. Heating with an electric plate

Cooking with the heat storage system is equivalent to putting a pot on a plate maintained at a constant temperature of around 215°C. Thus, to check the influence of the quality of the hot surface, a boiling test with a standard electric heating plate was run. The temperature of the plate is controlled using a sensor which automatically maintains the temperature between 213 and 217°C during the whole experiement (Figure 5). The sensor is placed under the heating plate, another one on the top verifies that both temperatures are similar.

Figure 5: Modified heating plate - Constant temperature

According to Figure 6, it takes around 16 minutes to boil water in this configuration, more than 2 times less than using the heat storage unit. The contact between the pot and the plate is then a major issue which can drastically improve heat transfer to the cooking vessel.

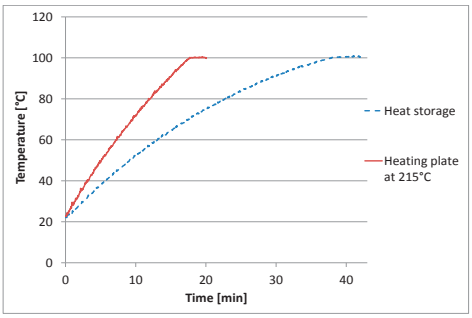

Figure 6: Comparison of boiling tests at constant hot plate temperature, with different contact qualities

4.3. Frying experiment

A frying experiment was conducted in order to collect experience regarding frying at constant temperature. A piece of meat (125 grams, 2 cm thick) is placed in a pan containing 30 ml of olive oil and sensors are installed (Figure 7). The storage unit is charged until the salts melt, then we put the pan on the top plate and start recording the temperatures in the olive oil and in the middle of the meat (Figure 8).

The temperatures of the oil and the meat are recorded as a function of the time until reaching a temperature of 80°C in the meat (Figure 9). The middle of the meat reaches the cooking

Figure 7: Installation of the thermocouple in the pan

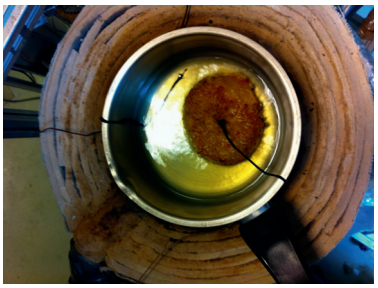

Figure 8: Frying experiment

temperature (over 71°C to kill Salmonella[23]) in less than 20 minutes (it was not turned during the frying). With improved surface contact, this time will be reduced and in the range of acceptable times for food preparation.

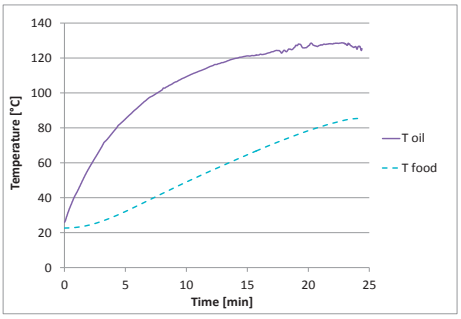

Figure 9: Frying experiment results

5. Simulations work

The simulations will provide a better understanding of the experiments.

5.1. Modeling of the SK14

A spreadsheet is programmed to simulate the temperature of the water. The pot receives energy from the sun following the parameters below. A coefficient is applied on the energy flux reflected by the parabola to correct the inaccuracy of the shape of the parabola [24]. The data are estimated and adapted from values from specialized websites or relevant articles[25, 20] The losses by radiation and convection (wind speed: 5 m/s for this experiment) are considered. The settings in the simulation are the following:

SK14 parabola:
- Area : $S = 1.54$ m2
- Reflection coefficient: $\gamma_p = 0.75$
- Corrector coefficient: $\beta_p = 0.65$

Steel pan:
- Absorption coefficient: $\alpha_p = 0.36$
- Emissivity: $\epsilon = 0.4$
- Diameter: $d = 17$ cm
- Height: $z = 8.5$ cm

External boundary conditions:
- Average insolation: $\phi = 850$ W/m2
- Atmospheric temperature: $T_a = 23.3$°C
- Wind speed: $v = 5$ m/s

T_w is deduced from this formula[26]:

$$T_w(t+1) = \frac{\gamma_p \beta_p \alpha_p S\phi - (\phi_c + \phi_r)}{mC_p} + T_w(t) \tag{1}$$

(1) is issued from the energy balance:

$$mC_p \Delta T = \phi - \phi_c - \phi_r \tag{2}$$

To estimate the losses by radiation, the formula used is the Stefan-Boltzmann equation ([26], Chapter 13):

$$\phi_r = \epsilon \sigma S_{pan}(T_w^4 - T_a^4) \tag{3}$$

Concerning the losses by convection ϕ_c, the convective coefficient h is deduced from the Reynolds and Nusselt numbers. ([26], Chapter 9, pp.510):

$$Re = \frac{vL}{\nu} \tag{4}$$

$$Nu = C.Ra^{\frac{1}{4}} \tag{5}$$

$$h = \frac{\lambda Nu}{L} \tag{6}$$

$$\phi_c = hA(T_w - T_a) \tag{7}$$

C=0.27 for the bottom of the pot (lower surface); C=0.59 for the sides of the pot; C=0.54 for the top of the pot([26], Chapter 9, pp.511).

The following graph (Figure 10) shows the evolution of the temperature as a function of time for the water heated with the SK14. The boiling time is 32 minutes for 1 liter of water, starting at 13°C.

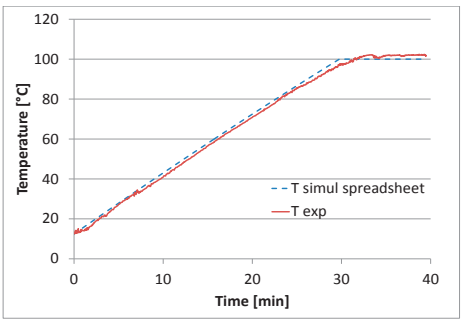

Figure 10: SK14 modeling

5.2. Simulation of the heat storage-based system

For this case, the simulation aims at predicting the temperature evolution of the storage unit and thus the temperature of the cooking plate. Knowing this temperature, it is possible to estimate the power transferred from the storage unit to the pot, and thus the temperature of the water as a function of time. Calculations were done considering that the storage unit has the following characteristics[15]:

Total mass: $m_{stor} = 10.44$ Kg
Composition (weight percentage):
- Steel: 26.1%
- Solar salts: 15.5%
- Duratherm 630 oil: 39.4%
- Aluminum : 18.9%

The estimation of the storage temperature is done considering the losses through the insulation ([26], Chapter 3) (in addition to the energy transmitted to the pot):

$$\phi_i = \frac{2\pi\lambda L}{ln(\frac{R_{ext}}{R_{int}})}(T_{storage} - T_a) \tag{8}$$

Losses from radiation and natural convection from the side of the plate not covered by the pot are estimated using formulas (3) and (7). For natural convection, the new convective coefficient h is calculated using the correlations (5) and (6) coupled with (7) using C=0.54 for the top of the storage not covered by the pan and the top of the pot; and C=0.59 for the sides of the pan ([26], Chapter 9, pp.511).

For the energy transmitted to the pot, we consider that the thermal resistance R_{th_p} of the pan is 0.865 W/K. This value is determined experimentally due to the difficulties determining a theoretical thermal resistance because of the non-optimal contact between the pan and the hot plate.

$$\phi_p = \frac{(T_{plate} - T_w)}{R_{th_p}} \tag{9}$$

Thereby, knowing the weight and the heat capacity of water, it is possible to determine the evolution of temperature as a function of time. From the energy balance:

$$mC_p\Delta T = \phi_p - \phi_r - \phi_c \tag{10}$$

where Q is the heat flux from the storage, we get then:

$$T_w(t+1) = \frac{(\phi_p - (\phi_c + \phi_r)).\Delta t}{m.C_p} + T_w(t) \tag{11}$$

where ϕ_r and ϕ_c are the losses from radiation (new computation from (2)) and natural convection from the pan[26].

Another simulation used Comsol software to visualize the temperature distribution in the system. The content of the vessel is modeled by a water layer (represented by a solid with high thermal conductivity to simulate the convection inside the water), an air layer and a lid. The storage is represented with aluminum cylinders containing melting salt, and oil. The insulation is represented as well. The Comsol simulation shows that the temperature into the storage is still high and quite uniform (Figure 11, after 25 minutes of heating).

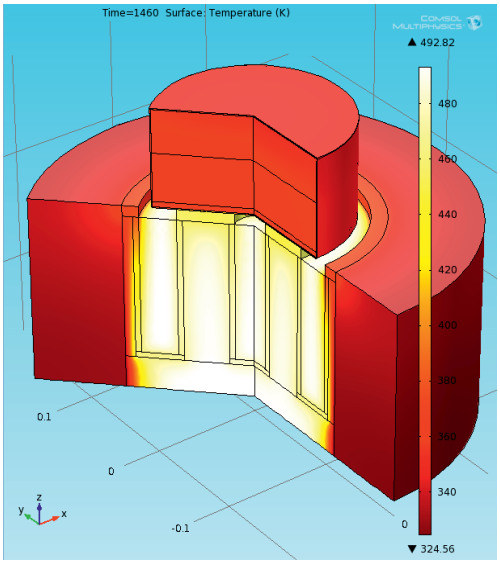

Figure 11: Comsol simulation - Time = 25 min

5.2.1. Water temperature - Comparison between experiment and simulations

The results obtained by the spreadsheet simulation and Comsol are plotted in Figure 12. The two simulations fit the experimental results and validate our hypothesis.

5.2.2. Heat storage temperature

According to the simulation, the temperature decreases but stays higher than 190°C until the boiling point. Note that the salts are then in theory solidified. In this simulation we used one average specific heat over 210°C (to include the latent heat from the salts) and another below 210°C. It is then possible to see the theoretical end of the phase change on this graph; and the Comsol simulation revealed a flat curve when the salts finished their solidification after about 24 minutes.

5.3. Frying experiment simulation

Using the same vessel as previously, the same properties are kept in this new simulation concerning the heat extraction between the plate and the pot, likewise the losses on the sides of the

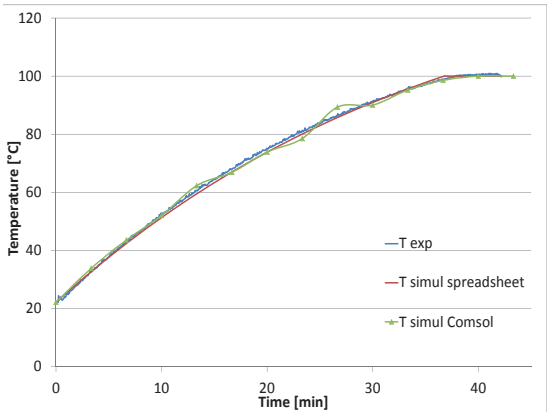

Figure 12: Simulation of the heat storage system

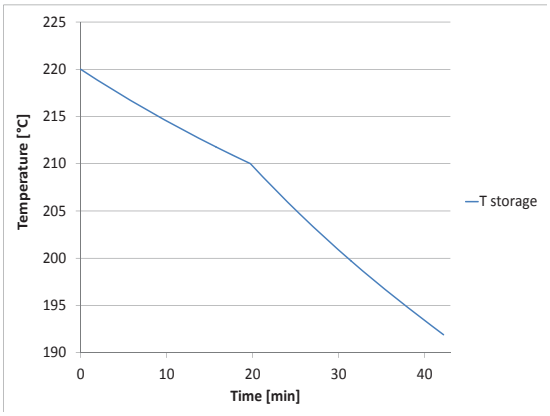

Figure 13: Behavior of the storage unit during discharging

pan by radiation and convection[26].

$$\phi_p = \frac{T_{plate} - T_{oil}}{R_{th_p}} \tag{12}$$

The following gives the characteristics concerning the meat and the olive oil:
Olive oil:
$C_{p_{olive}} = 1970$ J/kg.K
$\rho_{olive} = 900$ Kg/m3
$\lambda_{olive} = 0.17$ W/m.K
Meat:
$C_{p_m} = 3500$ J/kg.K

$\rho_m = 1060$ Kg/m^3
$\lambda_m = 0.5$ W/m.K
$d_m = 10.5$ cm
$h_m = 1.5$ cm

The formula used to estimate the heat transferred to the meat is[26]:

$$\phi_{meat} = \frac{T_{oil} - T_{meat}}{\frac{e}{\lambda_{olive}.A_{pan}} + \frac{h_m/2}{\lambda_m.A_m}} \tag{13}$$

The model considers a thin layer e of 1 mm of olive oil between the bottom of the pan and the piece of meat. Thus, the energy is transferred to the meat by conduction through two thermal resistances in series: the layer of olive oil and half of the meat thickness. A Comsol simulation was conducted to visualize the heat transfer.
The next Figure (14) shows a comparison between the experimental results and the two simulations.

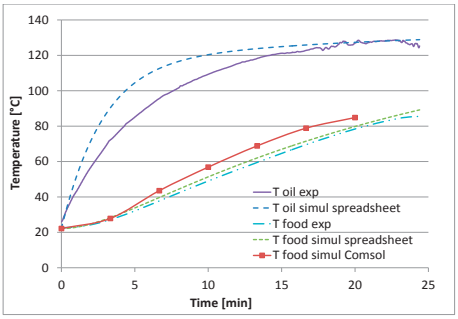

Figure 14: Frying comparison

According to the simulation results it is a relevant hypothesis to consider the thermal resistance of the food.

The Comsol simulation (Figure 15) shows the importance of the thermal resistance of the food, according to the gradient temperature in it. Turning the meat during frying will obviously optimize the cooking time and increase the quality of the cooking.

6. Interpretation of the results

Times to reach boiling point of one liter of water have been compared for cooking in the sun with the standard SK14 solar parabolic dish and for cooking on top of a oil and salt based heat storage (surface temeprature about 215°C). The prototype storage unit gave 25% longer cooking times than the SK14. Experiments with a smoother heat transfer surface gives 55% shorter times

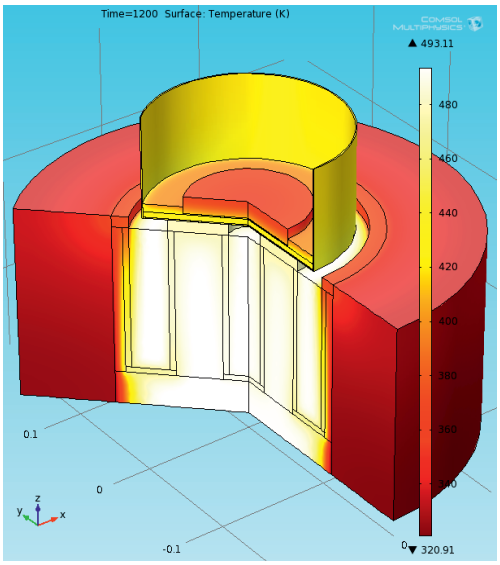

Figure 15: Comsol simulation - Time = 20 min

than the original surface.
Frying tests on the storage show acceptable food preparation times.

The heat transfer problems have been modelled and a tuning of heat transfer coefficients gives good correspondance with experiments for both a point model (spreadsheet) and for a 2D model (Comsol).

7. Conclusion

The current heat storage is slower than the SK14 for boiling water even with a standard pot (27 min for the SK14 against 38 min for the heat storage). However, the quality of the heat transfer can be significantly improved with an amelioration of the contact surface of the heat storage.
The current surface is not flat and a comparison with a perfectly flat surface is done. According to the experiments conducted with an electrical plate at constant temperature, it is then possible to boil water much more faster than with the SK14 (The boiling time is reduced to 16 min with an optimal contact). Such a system will have the advantage of cooking faster and being operational even without sunshine, as long as it is charged.
Concerning frying, the system already has useful frying time and is competitive to conventional heating systems. A solar cooker based on heat storage is a concept which can be developed and used in a sustainable way, knowing that it is possible to reach the performance of conventional direct solar cookers.

References

[1] H. Tabor. A solar cooker for developing countries. *Solar Energy*, 10:153–157, 1966.

[2] K. Schwarzer and M.E. Vieira da Silva. Characterisation and design methods of solar cookers. *Solar Energy*, 82:157–163, 2008.

[3] N. Nahar. Performance and testing of an improved hot box solar cooker. *Energy conversion and management*, 30:9–16, 1990.

[4] N. Nahar. Performance and testing of a hot box solar cooker. *Energy conversion and management*, 44:1323–1331, 2003.

[5] C.W. Foong, O.J. Nydal, and J. Lovseth. Investigation of a small scale double-reflector solar concentrating system with high temperature heat storage. *Applied Thermal Engineering*, 31:1807–1815, 2011.

[6] N.L. Panwar, S.C. Kaushik, and S. Kothari. State of the art of solar cooking: An overview. *Renewable and Sustainable Energy Reviews*, 16:3776–3785, 2012.

[7] A. Munir, O. Hensel, and W. Scheffler. Design principle and calculations of a Scheffler fixed focus concentrator for medium temperature applications. *Solar Energy*, 84:1490–1502, 2010.

[8] M. Mussard, E. Vaujany, and O.J. Nydal. Heating of an oil-based heat storage with a low-cost small-scale solar parabolic trough. In *Proceedings of the Eurosun conference in Opatija, Croatia*, 2012.

[9] M. Mussard and O.J. Nydal. Charging of a heat storage coupled with a low-cost small-scale parabolic trough for cooking purposes. *Solar Energy*, 10.1016/j.solener.2013.06.013, 2013.

[10] J. Rapp and P. Schwarz. Construction and improvement of a Scheffler reflector and thermal storage device. *Available at: http://www.digitalcommons.calpoly.edu/, last access: 20/11/12*, 2010.

[11] S.D. Sharma, T. Iwata, H. Kitano, and K. Sagara. Thermal performance of a solar cooker based on an evacuated tube solar collector with a pcm storage unit. *Solar Energy*, 2005.

[12] S.D. Sharma, D. Buddhi, R.L. Shawhney, and A. Sharma. Design and development and performance evaluation of a latent heat storage unit for evening cooking in a solar cooker. *Energy Conversion and Management*, 2000.

[13] A. Mawire, M. McPherson, R.R.J. van den Heetkamp, and S.J.P. Mlatho. Simulated performance of storage materials for pebble bed thermal energy storage (tes) systems. *Applied Energy*, 86:1246–1252, 2009.

[14] A.A. El-Sebaii, S. Al-Heniti, F. Al-Agel, A.A. Al-Ghamdi, and F. Al-Marzouki. One thous and thermal cycles of magnesium chloride hexahydrate as a promising pcm for indoor solar cooking. *Energy Conversion and Management*, 2011.

[15] M. Mussard and O.J. Nydal. Comparison of oil and aluminum-based heat storage charging coupled with a low-cost small-scale solar parabolic trough. *Applied Thermal Engineering*, 58:146–154, September 2013.

[16] A. Mawire, M. McPherson, and R.R.J. van den Heetkamp. Simulated energy and exergy analyses of the charging of an oil-pebble bed thermal energy storage system for a solar cooker. *Solar Energy Materials and Solar Cells*, 2008.

[17] A. Harmim, M. Boukar, and M. Amar. Experimental study of a double exposure solar cooker with finned cooking vessel. *Solar Energy*, 2008.

[18] H.M.S Hussein, H.H.El-Ghetany, and S.A. Nada. Experimental investigation of novel indirect solar cooker with indoor pcm thermal storage and cooking unit. *Energy conversion and management*, 49:2237–2246, 2002.

[19] D. Buddhi, S.D. Sharma, and A. Sharma. Thermal performance evaluation of a latent heat storage unit for late evening in a solar cooker having three reflectors. *Energy conversion and management*, 2003.

[20] A. Chandak, P.M. Suryaji, and S.K. Somani. Comparative analysis of SK14 and Prince-15 solar concentrators. *Proceeding of the world congress of engineering*.

[21] Duratherm Extended Life Fluids. Duratherm 630. *Available at: http://www.heat-transfer-fluid.com, last access: 20/11/12*, 2012.

[22] W. Kays, M. Crawford, and B. Weig. *Convective Heat and Mass Transfer, 4th edition*. McGraw-Hill Education, New York, 2005.

[23] www.meatandsausages.com/sausage-making/cooking-meat, last access 20/06/13.

[24] A. Valan Arasu and T. Sornakumar. Design and manufacture and testing of fiberglass reinforced parabola trough for parabolic trough solar collectors. *Solar Energy*, 2007.

[25] The engineering toolbox. Emissivity coefficients of some common materials. *www.engineeringtoolbox.com, last access: 06/12/12*.

[26] Y. A. Cengel. *Heat and Mass Transfer, 3rd edition*. McGraw-Hill Science/Engineering/Math, New York, 2007.

G. Solar cooker with heat storage at high temperature: charging experiments and simulations

Maxime Mussard

To be presented at the ISES Solar World Congress, Cancún, Mexico.
November 2013.
Accepted for publication in Energy Procedia, 2013.

Available online at www.sciencedirect.com

SciVerse ScienceDirect

Energy Procedia 00 (2013) 000–000

Energy Procedia

www.elsevier.com/locate/procedia

2013 ISES Solar World Congress

Solar cooker with heat storage at high temperature: charging experiments and simulations

Maxime Mussard*

NTNU, Department of Energy and Process Engineering, Kolbjørn Hejes vei 1D, Trondheim 7491, Norway

Abstract

A self-circulating loop is coupled with a heat storage and a solar parabolic trough for charging experiments. The loop is filled with thermal oil (Duratherm 630). The parabolic trough focuses the energy on an absorber tube. Based on experimental results of the charging of a heat storage, a numerical upscaling of the system is made using Matlab. By numerically improving the coating of the absorber, modifying the pipe diameters and optimizing the size and the content of the storage, an optimal system can be virtually designed. The storage is originally based on aluminum cylinders filled with nitrate salts immersed in the heated oil coming from the self-circulating loop. The salts provide latent heat to the heat storage (melting temperature: 215 to 225°C). The absorber is originally insulated with an air layer; an evacuated tube is then numerically tested. The vacuum provides a much better insulation: it allows then a greater potential for heat storage. However, overheating of the oil in the absorber is an issue and the design of the pipes needs then to be modified (increase of diameter).
A new heat storage based on tin is virtually designed, with larger heat storage potential. The diameters of the pipes are slightly increased again to speed up the flow and reduce overheating.

Selection and/or peer-review under responsibility of ISES

Keywords: solar cooking ; heat storage ; latent heat

1. Introduction

Due to the increasing economic and environmental tensions on fossil fuels and biomass, solar energy becomes more and more attractive throughout the years. It is especially true in the southern countries where sun is available; deforestation becomes a major problem and the income per capita remains low. Solar cooking is an interesting option for spreading solar energy: indeed, cooking is one of the basic needs of humankind and represents an important source of energy consumption. Using solar cooking in

* Corresponding author. Tel.: +47 735 93899;
E-mail address: maxime.mussard@ntnu.no.

sunny areas may then help to reduce poverty and deforestation, gain significant time usually spend on collecting wood, and reduce health diseases due to indoor smoke.
Solar cookers have been deeply investigated during the last decades; the most common principle is direct cooking with boxes [1] or parabolas [2]. Direct cooking is powerful and sufficient when there is sunshine; however, cooking occurs very often during the evening when the sun is already down.
Using a heat storage can help to make a solar cooker competitive even by night: by storing heat during the day, the system enables cooking by night. This concept has been developed with different systems [3, 4]. However, getting a cheap, robust and user friendly system which can store energy over 200°C (to enable both boiling and frying) is more challenging. Experiments made by Mussard [5] shows the ability for a parabolic trough to charge a storage over 220°C with an air layer insulating the absorber.

2. Objectives

From a charging experiment [5], the potential of a small-scale solar cooker is tested using an improved simulation tool. By first testing the model with a selective coating and then with larger pipes to reduce friction, and finally with an evacuated tube around the absorber it is possible to expand the storage to its theoretical limits and conclude about the heat storage potential of such a system. A larger storage allows to store much more energy at constant temperature and increases drastically the cooking potential of the system.

3. Description of the system

3.1. Self-circulation loop

The system is the same than described in precedent articles [6]. The system works by self-circulation: the oil circulates due to the density difference of cold and hot oil.

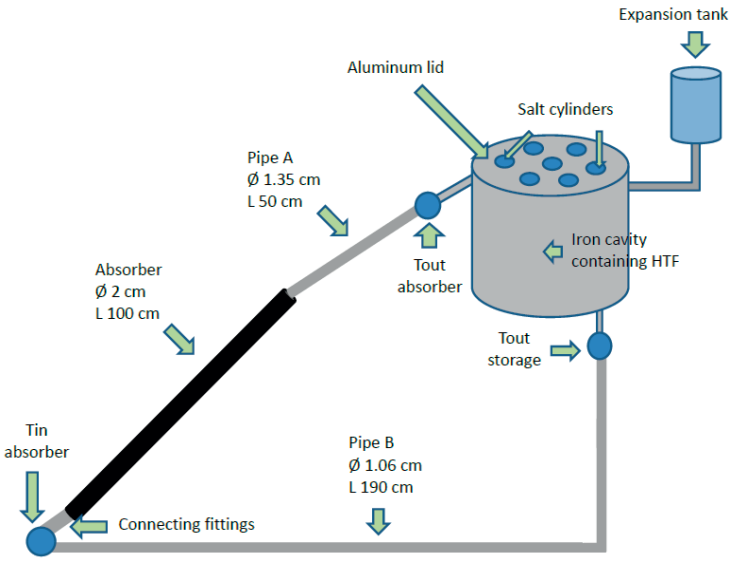

Fig. 1. Schematic presentation of the self-circulating loop with piping dimensions

Concerning the experiment, the loop is filled with Duratherm 630, the total oil volume in the pipes is about 0.6 liters, and the total oil volume (pipes + storage) is 5.45 liters. For the simulations, the oil is supposed to have the same characteristics, even if the viability of the oil at these temperatures is not proved.

Fig 1 shows a schematic view of the loop connected to the oil-based storage [6], with corresponding pipe dimensions.

3.2. Heat storage

As described previously, the storage of the experiment is made of aluminum cylinders filled with nitrate salts which provide latent heat at about 220°C [6]. An expansion tank is connected to the top of the storage.

The cavity is then filled with oil and the salt cylinders are immersed into it (Fig 2).

Fig. 2. View of the top of the storage – Aluminum and salt cylinders

4. Original experiment and first numerical model

4.1. Experiment

A charging experiment was made under sunny conditions and the results are shown on Fig 3. The simulation results from the model by Mussard [5] are plotted as well. The system shows ability to reach 230°C.

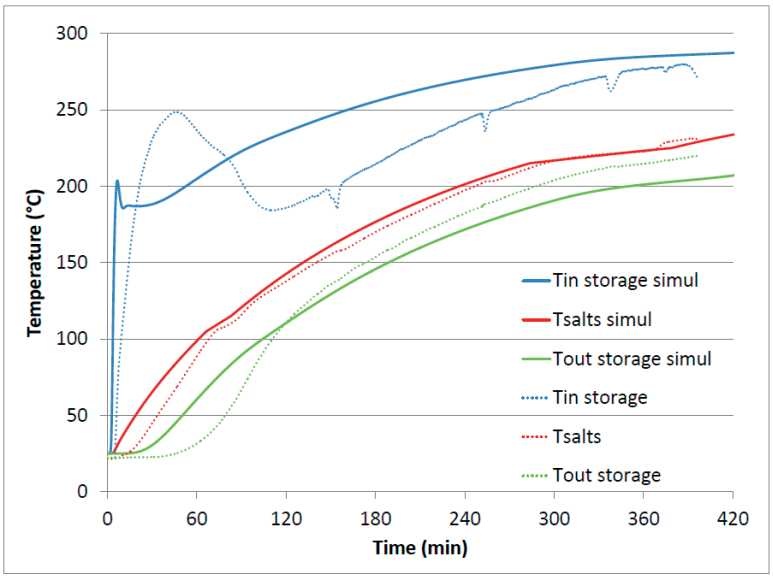

Fig. 3. Charging experiment and simulation

4.2. Improvements of the current system using the simulation tool

The system is improved by optimizing the coating, and increasing the diameter of the smallest pipes.

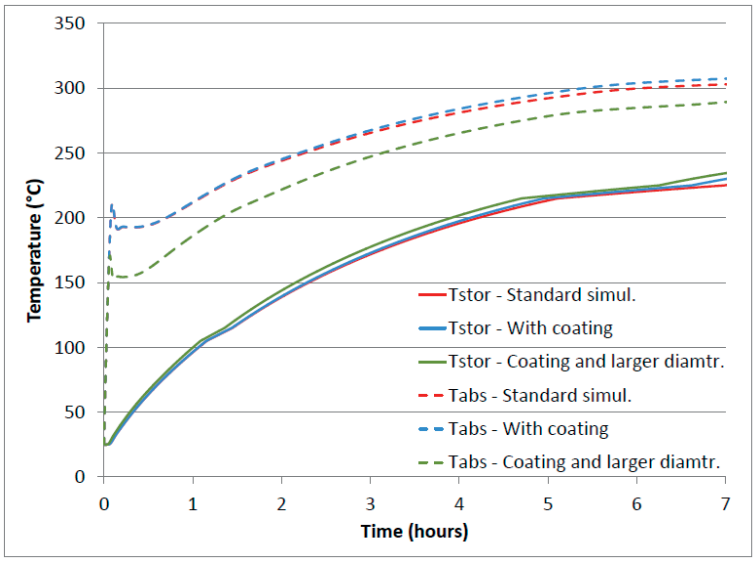

Fig. 4. Simulations of the improvements of the system

Concerning the coating, the original emissivity was estimated at 0.8. A selective coating may reduce the emissivity to about 0.03 [7]. The simulation is then run using this data. A slight improvement of the performance can be observed, but remains small due to the relatively low temperature in the absorber compare to other solar installations.

The diameters of the two short tubes at the inlet and outlet of the storage are then virtually increased from 10 to 12 mm, and from 8 to 12 mm. The diameter of Pipe B is increased from 10.6 to 13.5 mm. By increasing the diameter, the performance is slightly increased despite the potentially higher thermal losses along the pipes. Indeed, the reduction of the friction increases the flow rate and explains as well the lower temperature in the absorber. Optimizing the diameter of the pipes may be then an interesting option to avoid oil overheating.

The results are shown on Fig 4.

5. Improvement of the model using an evacuated insulation around the absorber

5.1. Potential of evacuated insulation

An experiment has been started with the current prototype coupled with an evacuated insulation, and the temperature increase of the storage the first minutes was promising. Unfortunately, the performance decreased experiment after experiment: a hypothesis could be the deposit of burned oil along the pipes. The experimental setup is then most probably underscaled for this kind of absorber insulation. However, by using the simulation tool, it is possible to have an idea of the theoretical behavior of the system under these conditions. By supposing that the oil could stand the temperatures reached, we can see that the storage can be charged 2 times faster than with the air insulation, in less than 3 hours (Fig 5). Vacuum insulation is then a critical factor for optimizing the efficiency of the system. It is possible as well to visualize the positive effect of enlarged pipe diameters on the temperature of the absorber.

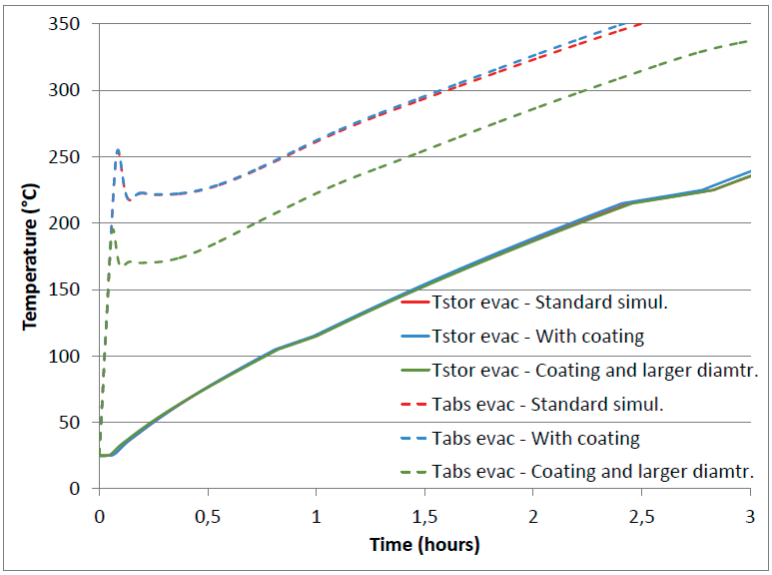

Fig. 5. Original system simulated considering an evacuated insulation around the absorber

5.2. Upscaling of the storage

As seen previously, evacuation allows a charging in less than 3 hours. So with a much higher heat storage potential, it is expected to store a very important amount of energy during a full sunny day (8 to 9 hours).

A new storage is virtually design, the diameter is increased from 20 to 25 cm, the height remains 20 cm. The new storage has a volume of 9.8 liters: 3.3 liters of tin (high volumetric latent heat of 456 kJ/L [8]) and the rest filled with oil. The heat storage potential above 220°C is about 5 times larger than the previous storage. The original storage proved to be good enough to cook for about 2 people [9], we can then expect a cooking potential for up to 10 people with such storage potential. The simulation proves that charging such a storage with the same collector and an evacuated tube (and selective coating) is possible. By increasing of 2 mm the diameter of all the pipes except the absorber (blue lines), it is theoretically possible to reduce the temperature in the absorber while slightly affecting the performance of the system. All the data are displayed on Fig 6.

Furthermore, tin has numerous advantages: it is chemically much more stable than the nitrate salts, the volumetric latent heat is higher, the volumetric sensible heat below the melting point is lower (so the preheating is faster) and the heat conductivity is important. However, the price may be prohibitive and the weight makes it very difficult to move after installation. Further investigations must be lead to carefully optimize such a system.

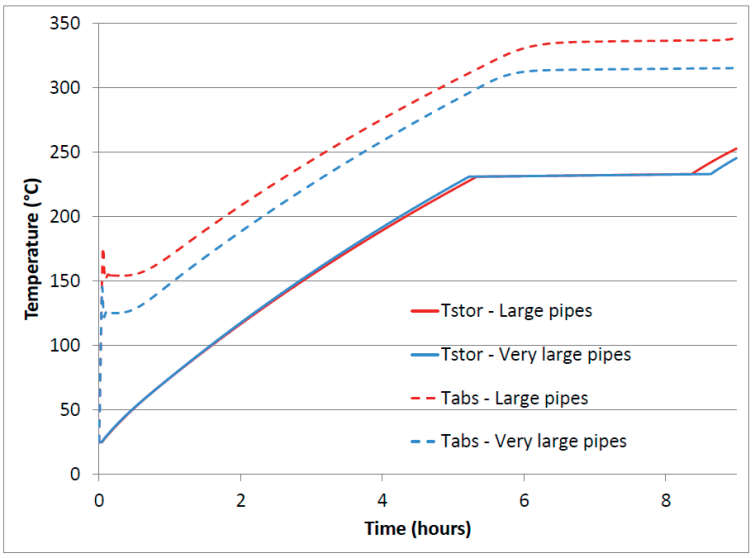

Fig. 6. Simulation of the upscaling of the storage using tin

6. Conclusion

Starting from an experimental test, the solar cooker coupled with a parabolic trough and a heat storage shows a great potential. Experiments have then been tried with the original setup and an evacuated tube, but the system seems underscaled and a more careful optimization is necessary before running new experiments. However, by using a simulation tool, the efficiencies of different improvements are tested. If the selective coating does not improve drastically the efficiency of the system, the use of an evacuated tube around the absorber reduces by a factor 2 the charging time for the original storage. Considering this, a larger storage is virtually designed. By running the system during a full sunny day, it is theoretically possible to load 5 times more energy than previously. To avoid overheating of the oil, an advanced optimization of the diameter of the pipes and/or the absorber tube should be done, to regulate the mass flow such that the critical temperature (auto-ignition point) is never reached.

References

[1] Nahar N. Performance and testing of an improved hot box solar cooker. *Energy Conversion and Management* 1990;**30**:9–16.

[2] Gallagher A. A solar fryer. Solar Energy 2011;85:496-505.

[3] Schwarzer K, Vieira da Silva M. Characterisation and design methods of solar cookers. *Solar Energy* 2008;163:82–157.

[4] Rapp J, Schwarz P. Construction and improvement of a Scheffler reflector and thermal storage device. Available at: *www.digitalcommons.calpoly.edu/*, 2010; last access: 03/05/13.

[5] Mussard M, Nydal O. Charging of a heat storage coupled with a low-cost small-scale parabolic trough for cooking purposes. *Accepted in Solar Energy*.

[6] Mussard M, Nydal O. Comparison of oil and aluminum-based heat storage charged with a small-scale solar parabolic trough. *Applied Thermal Engineering* 2013;**58**:146-154.

[7] *ASHRAE Handbook Fundamentals - IP Edition*. American Society of Heating, Refrigerating and Air-Conditioning Engineers, Inc. Atlanta, GA. 2010.

[8] Mussard M, Nydal O. Assessments of the thermal storage potential of sensible and latent heat-based systems for solar domestic applications. *Proceedings of the 7th International Renewable Energy Storage Conference, Berlin, Germany.* 2012.

[9] Mussard M, Gueno A, Nydal O. Experimental study of solar cooking using heat storage in comparison with direct heating. *Submitted to Solar Energy.*